Aspects on Cardiac Pumping

Carlsson, Marcus

2007

Lund University, Faculty of Medicine Doctoral Dissertation Series
2007:47

Aspects on Cardiac Pumping

MARCUS CARLSSON, M.D.

LUND UNIVERSITY

Doctoral Thesis
2007

Department of Clinical Physiology
Clinical Sciences, Lund, Faculty of Medicine
Lund University, Sweden

Faculty opponent
Prof Anders Waldenström, M.D., Ph.D., Umeå University, Umeå, Sweden

ISSN 1652-8220 • ISBN 978-91-85559-25-1

The public defense of this thesis for the degree Doctor of Philosophy in Medicine will, with due permission from the Faculty of Medicine at Lund University, take place in Föreläsningssal 1, Lund University Hospital, on Friday, 16 March 2007, at 09.00.

Cover:
A three dimensional image of the heart reconstructed from MR images of a normal subject. The contours of the pericardium in open net, the epicardial contours of the left ventricle in red and right ventricle in green. Opaque surfaces show the contours in end diastole and transparent surfaces the contours in end systole.

Department of Clinical Physiology
ISSN 1652-8220 Clinical Sciences, Lund, Faculty of Medicine, Lund University
ISBN 978-91-85559-25-1 SE-221 00 LUND, Sweden

A full text electronic version of this thesis is available at
http://theses.lub.lu.se/postgrad

Typeset using LaTeX and the template lumedthesis.cls ver 1.1,
available at http://www.hedstrom.name/lumedthesis
Printed by: KFS AB, Lund, Sweden

marcus.carlsson@med.lu.se

Hojotoho! Hojotoho!
Heiaha! Heiaha! Hojotoho! Heiaha!
—Die Walküre, Richard Wagner

Contents

List of Publications

This thesis is based on the following papers, which in the text will be referred to by their Roman numerals.

I. **Carlsson M**, Cain P, Holmqvist C, Stahlberg F, Lundback S, Arheden H. Total heart volume variation throughout the cardiac cycle in humans. *Am J Physiol Heart Circ Physiol.* 2004;287:H243-250.

II. **Carlsson M**, Rosengren A, Ugander M, Ekelund U, Cain PA, Arheden H. Center of volume and total heart volume variation in healthy subjects and patients before and after coronary bypass surgery. *Clin Physiol Funct Imaging.* 2005;25:226-33.

III. **Carlsson M**, Ugander M, Mosen H, Buhre T, Arheden H. Atrioventricular Plane Displacement is the Major Contributor to Left Ventricular Pumping in Healthy Adults, Athletes and Patients with Dilated Cardiomyopathy. *Am J Physiol Heart Circ Physiol.* 2006:01148.2006.

IV. **Carlsson M**, Ugander M, Heiberg E, Arheden H. The Quantitative Relationship between Longitudinal and Radial Function in Left, Right and Total Heart Pumping in Humans. *Submitted.*

V. **Carlsson M**, Ugander M, Arheden H. The Total Heart Volume Increases Prior to the Conclusion of Systolic Ventricular Ejection and Decreases during Atrial Contraction in Humans. *Manuscript.*

Summary

Cardiac pumping physiology is important for understanding the pathophysiology of patients with cardiac disease. MRI gives the opportunity to measure volumes and flow non-invasively with high accuracy and precision. This thesis examines some aspects on cardiac pumping physiology. Study I showed that the total heart volume in humans decreases during systole by ∼8 % (range 5-11 %), and anatomically identified the major outer volume variations to occur around the AV-plane with a left-side predominance. Also, a new method for measuring total heart volume variation (THVV) by MRI flow quantification was developed and validated against cine measurements. Study II showed that the THVV is similar in patients before and after cardiac bypass surgery compared to healthy subjects. Furthermore, study II also showed that the movement of the center of volume of the heart during the cardiac cycle, in both healthy individuals and patients, describes a well-defined loop in three-dimensional space with ∼2 mm between the extreme points. This loop is called the center of volume variation, COVV. After coronary-bypass surgery, however, intra-individual COVV approximately doubled, possibly related to the paradoxical septal movement following cardiac surgery. Study III showed that longitudinal AV-plane displacement (AVPD) is the primary contributor to left ventricular (LV) pumping, accounting for ∼60 % of the stroke volume (SV) in healthy subjects and that this does not differ in athletes or in patients with dilated ventricles. Study IV showed that radial function of the ventricles explains over 80 % of the THVV during the cardiac cycle. The longitudinal component of right ventricular (RV) pumping is ∼80 % and the difference compared to the LV is explained by the larger AVPD of the RV. Study V identified and quantified a previously unknown increase in total heart volume before the end of systolic ejection. This total heart volume increase or late ejection filling volume (LEFV) into the atria was ∼11 ml or ∼18 % of THVV, with no difference between the left and right side of the heart. This volume might be important for understanding the coupling of systolic to diastolic function. Furthermore, the decrease in total heart volume caused by flow from the heart generated by atrial contraction (the atrial wave reversal volume, AWRV) was quantified to be ∼7 ml or ∼11 %

of THVV. Thus, the heart is largest before atrial contraction prior to the end of diastole and smallest before the end of systole.

In summary, this thesis has explained the total heart volume variations throughout the cardiac cycle and quantified the contribution of the AV-plane to ventricular pumping.

Populärvetenskaplig sammanfattning

Förståelse av hjärtats pumpförmåga är av yttersta vikt för att kunna behandla patienter med hjärtsjukdom, framförallt hjärtsvikt. Studier av hjärtat har av naturliga skäl framförallt gjorts med öppen bröstkorg eller med hjärtat uttaget ur kroppen, och detta påverkar hjärtats pumpning. Magnetresonans-kameran gör det möjligt att avbilda hjärtat i alla delar av hjärtcykeln samt att mäta flödet i kärlen till och från hjärtat. Denna avhandling har studerat hur och varför hjärtat varierar i volym under hjärtcykeln samt kvantifierat de olika sätt som hjärtats kammare arbetar. Delarbete I visade att hjärtats yttre volymförändring under hjärtcykeln hos friska frivilliga var c:a 8 % och varierade från 5-11 %. Både flödesmätning och volymsbestäming av hjärtat över hjärtcykeln gav samma resultat. Den yttre volymförändringen är låg jämfört med hur mycket blod som tömmer sig ur kamrarna men det förklaras av inflöde av blod till förmaken. Vid jämförelse mellan höger och vänster sida av hjärtat återfanns en större del (60 %) av den yttre volymförändringen på vänstersidan. Delarbete II visade att hjärtats yttre volymförändring hos patienter var i stort sett oförändrad före och efter kranskärlsoperation och skilde sig inte jämfört med friska. Dessutom visade studien att centerpunkten (volymcentrum) i hjärtat rör sig under en hjärtcykel i en loop som börjar och slutar på samma ställe. Loopen är c:a 2 mm mellan extrempunkterna. Denna rörelse skilde sig inte mellan friska och patienter men efter operation dubblerades rörelsen till c:a 4 mm. Delarbete III visade att 60 % av vänsterkammarens slagvolym genereras av den längsgående förkortningen av kammaren genom att basen av kammaren (AV-planet) förflyttas mot kammarspetsen under tömningsfasen. Detta mättes dels på friska frivilliga men också hos atleter på elitnivå och patienter med förstorade vänsterkammare och sänkt kammarfunktion. Det var ingen skillnad mellan grupperna i andelen slagvolym som orsakas av längsgående förkortning. Delarbete IV visade på motsvarande sätt som delarbete III att 80 % av högerkammarens slagvolym genereras av den längsgående förkortningen hos friska frivilliga. Dessutom kunde delarbetet visa att hjärtats yttre volymsförän-

dring till över 80 % kan förklaras av den radiella, kramande, kammarpumpningen. I delarbete V studerades när hjärtat är som störst och som minst. Hjärtats största volym inträffar före förmakskontraktionen då blod inte bara förflyttas från förmak till kammare, men också ut ur hjärtat som backflöde i venerna. Denna volym kvantifierades med flödesmätning på höger och vänster sida. Hjärtat är inte som minst vid slutet av systole utan börjar öka i volym före denna tidpunkt vilket beror på att inflödet av blod till förmaken är större än utflödet. Detta kan innebära att det finns en rörelseenergi i blodet på väg in i förmaket vid det tillfälle då klaffarna mellan förmak och kammare öppnas och detta kan vara en del i förklaringen till den snabba fyllnadsfasen. Dessa parametrar kan ge ny information för att förstå hjärtats pumpfunktion.

Sammanfattningsvis har denna avhandling visat hur hjärtat minskar i volym under kammarsystole samt att den främsta orsaken till detta är kamrarnas kramande radiella kontraktion. Hjärtats volymsvariation över hjärtcykeln har visat att hjärtat är som störst innan förmakssystole och som minst innan slutet av kammarsystole. Dessutom har AV-planets bidrag till de båda kamrarnas slagvolym kvantifierats.

Abbreviations

2ch	two chamber
4ch	four chamber
AVPD	atrioventricular plane displacement
AV-plane	atrioventricular plane
AWRV	atrial wave reversal volume
COV	center of volume
COVV	center of volume variation
CT	computed tomography
DCM	dilated cardiomyopathy
ECG	electrocardiogram
LA	left atrium
LEFV	late ejection filling volume
LV	left ventricle
LVOT	left ventricular outflow tract
LVSV	left ventricular stroke volume
MRI	magnetic resonance imaging
RA	right atrium
ROI	region of interest
RV	right ventricle
RVSV	right ventricular stroke volume
SA	short axis
SENSE	sensitivity encoding
SV	stroke volume
SV_{AVPD}	stroke volume generated by AVPD
$SV_{AVPD\%}$	the portion of the stroke volume generated by AVPD in percent of the SV
THV	total heart volume
THVV	total heart volume variation
VENC	velocity encoding

Chapter 1

Introduction

1.1 Cardiac pumping

It is essential to understand the mechanics of cardiac pumping in order to understand cardiovascular physiology and correctly interpret the pathophysiology of patients with cardiovascular disease. Heart failure is defined as the inability of the heart to deliver the cardiac output required by the body´s metabolism with sustained filling pressures.[1] Heart failure is relatively common and the incidence increases with age.[1] It is estimated that 10 million people have heart failure in Europe[2] and in Sweden alone 250 000 people,[3] the most common aetiology being coronary disease.[4] The prognosis is poor, despite modern pharmacotherapy. Half of the patients with heart failure will die within four years and among those with severe heart failure within one year.[2] In the Medicare system of the United States, heart failure cost more money than any other diagnosis.[5] Furthermore, modern research is often focused on understanding cellular and molecular physiology and pathophysiology, but the basic concepts of cardiac pumping on a macroscopic level are still not completely understood.[6] MRI can be used to accurately measure volume and flow, and this makes it possible to undertake detailed studies of cardiac function in humans.

Cardiac structure and the cardiac cycle

The heart is composed of myocardium which encloses four cavities, two atria and two ventricles. The pericardium encloses the myocardium. The atria are separated from the ventricles by the atrioventricular plane (AV-plane) which is a fibrous structure where the valves are inserted. The heart is divided into a right and left side, each having one atrium and one ventricle (Figure 1.1). The right atrium receives blood from the body through the two caval veins, the superior

caval vein receiving blood from the head, arms and thorax and the inferior caval vein receiving blood from the lower part of the body. The right ventricle delivers blood to the lungs through the pulmonary trunk. The blood from the lungs returns to the left atrium through the four pulmonary veins. The blood is ejected from the left ventricle to the aorta which transports blood to the systemic circulation. The resistance is four to five times higher in the systemic circulation compared to the pulmonary circulation. Therefore, the LV needs to generate higher pressures compared to the RV and hence the myocardium of the left ventricle is four to five times thicker than the right ventricular myocardium. The part of the myocardium facing the lumen is called the endocardium and the part farthest away from the lumen is called the epicardium. The heart is surrounded by the pericardium, composed of two layers which are lubricated by a small amount of pericardial fluid. This minimizes the friction of the movement of the heart against the pericardium.[7]

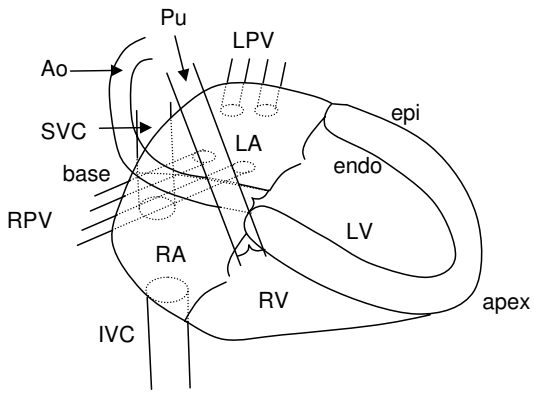

FIGURE 1.1 Schematic view of cardiac structures. Ao aorta, endo endocardium, epi epicardium, IVC inferior vena cava, LA left atrium, LPV left pulmonary veins, LV left ventricle, Pu pulmonary trunk, RA right atrium, RPV right pulmonary veins, RV right ventricle, SVC superior vena cava

The myocardium is composed of different layers and is often described as having three layers, an endocardial layer with longitudinal fibers, a thick midwall layer with circular fibers and an epicardial layer with longitudinal fibers.[8–10] Studies of ventricular structure have proposed that the myocardium of both ventricles

is a organized as a continuous muscle band oriented in loops.[11–13] Furthermore, the fibers from the apex to the base have been shown to be oriented in the shape of a helix and the transition of fibre angles from the epicardial left-handed helix to the endocardial right-handed helix has been shown to be smooth.[14–16]

Inner volume changes during the cardiac cycle

The volume changes of the individual chambers of the heart have been studied extensively and are illustrated in most physiology and cardiology textbooks.[17–21] Systole is the term used to describe the phase of contraction of myocardium causing emptying of blood and diastole is the term that describes the filling phase. Pressure differences drive blood flow. Myocardial contraction generates increased pressure when the valves are closed and the volume cannot be diminished, and this is called isovolumetric contraction. When the valves are open myocardial contraction also causes volume decrease as blood leaves the chamber. Systole and diastole of the atria and ventricles are separated in time. During ventricular ejection the atria are filled by blood, and this is called the reservoir function of the atria.[22–27] Ventricular diastole is characterized by an initial short isovolumetric relaxation followed by an early rapid filling phase and a subsequent later or atrial filling phase.[28] During the time between the early and late filling phases there is little flow into the ventricle. The relative contribution of the early and atrial filling phases changes with age and is affected by diastolic dysfunction.[29] The rate of the filling and emptying of the ventricles are well established measures of ventricular diastolic and systolic function, respectively.[29–34] The atria is described as conduits during the first part of diastole.[22–27,35] During this phase blood from the veins can pass through the atria to the ventricles because of the open AV-valves. However, most blood that enters the ventricles during the first part of diastole entered the heart during systole (the reservoir function). The last phase of ventricular diastole occurs during atrial systole and this is described as a booster function for the ventricles.[23,25] The effect of atrial contraction is a slight increase in atrial pressure and thus flow from the atria to the ventricles. However, the main effect of atrial contraction is a decrease in atrial volume mainly by shifting the AV-plane towards the base and thus increasing the volume of the ventricles. The contribution of atrial contraction in normal subjects is 10-20 % at rest but this atrial contribution to stroke volume increases linearly with heart rate during exercise.[36,37] Furthermore, recent studies have examined the three dimensional flow patterns within the heart[38–40] which have given new insights to the physiological consequences of the fluidic properties of the blood flowing through the heart. The location of the insertion of the pulmonary and caval veins into the heart contributes to the formation of a vortex within each atrium, and these vortices direct blood towards the AV-valves. According to Newton's third law, a generated force will have an equal

force in the opposite direction. The forces of the blood ejected through the aorta and pulmonary trunk are directed towards the AV-plane because of the sinuously looped atrioventricular arrangement in vertebrates. Thus, the enlargement of the atria is influenced by ventricular contraction which pulls the AV-plane towards the apex, but also by the opposite force directed from the AV-plane of the ejected blood through the aorta and pulmonary trunk. In diastole, the enlargement of the ventricles, or the return of the AV-plane, is facilitated by the momentum of part of the blood entering the ventricles directed towards the AV-plane.[36,40] Thus, there is an atrio-ventricular coupling of the inner volume displacement within the heart during the cardiac cycle and this is mediated by the AV-plane.

Outer volume changes during the cardiac cycle

Much less is known regarding outer volume changes of the heart compared to the volume changes of the individual chambers. Textbooks on cardiac physiology and pathophysiology often include illustrations of large outer volume variations from diastole to systole.[17,19] This may be an effect of the outer volume variations that are apparent during open heart surgery, or when observing isolated hearts in a Langendorff preparation. During surgery or Langendorff preparation, the systolic ejection of blood from the heart to the great arteries will result in a decreased volume of the ventricles which moves the pericardium inwards. This outer volume variation has been called total heart volume variation (THVV) because the volume of all structures within the pericardium is taken into account. The extent of THVV will have an impact on the efficiency of cardiac pumping. A large total volume change will result in energy loss through either displacement of surrounding tissues or induction of a pendular motion of cardiac tissue and blood.[41–44] Cardiac pumping would thus require energy in order to move, for example, lung and liver tissue. Studies of outer volume changes during the cardiac cycle within the intact thorax using different techniques have shown somewhat different results. In 1932, Hamilton and Rompf described a relative constancy of the total heart volume during the cardiac cycle in frogs, turtles and dogs.[43] Subsequent non-invasive investigations in cats, monkeys[45] and dogs[41,44] were concordant with this initial finding of a relatively constant total heart volume over the cardiac cycle. The observed outer volume variations of the heart have been proposed to be a measurement error.[41] Interestingly, Gauer used x-ray fluoroscopy and reported a 2 % larger systolic volume compared to the diastolic total heart volume in a cat before and after pooling of blood by increased g-forces.[45] Some authors[41,46] have referred to Gauer´s results as being in conflict with those of Hamilton and Rompf. Gauer concluded that systolic filling of the atria is larger in small animals compared to large animals such as humans and that this is coupled to the faster heart rates. This means that a larger THVV can be expected in larger species with

slower heart rates, for example humans, compared with the previously studied smaller species.

Investigations in humans using CT[47] and MRI in ventilated healthy subjects[48] have suggested that a volume variation of 8-13 % may occur between diastole and systole. However, recent work found a lower volume variation of 5 % using modern MRI techniques.[49] The explanation for the difference between the observations during open heart surgery and using non-invasive techniques has not been fully investigated. One potential mechanism may be the differences in the status of the pericardium. The role of the pericardium in interaction between the compartments of the heart has been debated.[50–55] However, it has been suggested that the negative pericardial pressure generated during systole is important for right atrial filling during systole, and that pericardiotomy lowers atrial systolic filling.[7] Also, a lower atrial systolic filling volume will result in an increased THVV. Recently, a study using MRI found a THVV of 13 % in a subject with congenital absence of the pericardium compared to the 5 % THVV in control subjects.[49] However, Hoffman showed that the THV remained relatively constant when airway pressure was increased and the THV was lower.[41] Thus, THVV was low even when the heart did not "fill out" the pericardium. Furthermore, the intrathoracic pressure within the closed chest as such may also have implications for THV constancy. In summary, the role of the pericardium for maintaining low THVV is not clear.

The center of volume variation (COVV) during the cardiac cycle will also affect cardiac efficiency but has been studied even less than the THVV. The COVV is a term used to describe the movement over time of the volumetric or geometrical center of a three dimensional structure. A constant THVV can be associated with a large COVV if the heart expands in one part and concomitantly decreases by the same volume in another part. The effect of COVV on cardiac pumping efficiency is apparent in the formula for calculating work.

$$\text{Work} = \text{Mass} \times \text{Acceleration} \times \text{Distance}$$

Distance traveled in this case is the COVV. Thus, work is performed when the center of volume of the heart is accelerated from one point to the other during each cardiac cycle. A constant or low COVV is thereby coupled to conservation of energy. Hoffman *et al* studied cardiac pumping and found a relative constancy of the COVV (called center of mass by the authors) using computed tomography in six volunteers.[47] They observed a COVV of 3 mm between end-diastole and end-systole along the left ventricular long axis. Studies in children with congenital heart disease found a small COVV at different stages of Fontan reconstruction[56,57] and no discernible pattern of movement in the COVV.

Longitudinal and radial function of the ventricles

The reduction of ventricular volumes during systole occurs by longitudinal and radial shortening of the ventricles,[58] which was already described by Harvey in the 17th century.[59] Even earlier work by da Vinci showed greater movement in the heart at the base compared to the midventricular part, and little movement at the apex.[60] Longitudinal function has been described in experimental studies[42,43,45] and the systolic longitudinal shortening of the ventricle has been shown to start during isovolumetric contraction.[61] The movement of the base of the ventricles has been shown by different techniques such as roentgen cinematography,[62,63] angiography[58] and ultrasound.[64] Also, in clinical echocardiography, the movement of the AV-plane measured by M-mode Doppler is used to assess global ventricular function and estimate left ventricular ejection fraction.[65–67] The notion that longitudinal function is an important part of left ventricular pumping is known from theoretical calculations. The EF would be <30 % and the shortening fraction ~12 % if there were only short-axis contraction without the contribution of longitudinal shortening.[8,68] Yet, left ventricular pumping is still described in modern textbooks on physiology and pathophysiology as the result of the radially diminishing diameter of the left ventricle.[17,19]

Figure 1.2 illustrates how to calculate the portion of the stroke volume generated by the longitudinal AVPD. Panel A shows the epicardial contour of a schematic LV with only longitudinal pumping. The broken lines indicate the position of the AV-plane in end systole. The stroke volume generated by the AVPD (SV_{AVPD}) is the volume basal to the position of the AV-plane in end systole, shown in grey.

Panel B shows the same ventricle as in A. d_1 denotes the largest diameter of the LV defined as the greatest epicardial area in a short axis plane. d_2 denotes the diameter at the position of the mitral valve. The grey region indicates the diameter (d_1) multiplied by the AVPD. This region is the same size as the grey region in A, see D below.

In panel C myocardium is added to the model. Myocardium reduces the inner contour of the ventricle but the volume of the myocardium is constant throughout the cardiac cycle. The myocardium is rearranged as it pulls the AV-plane towards the apex and therefore appears thickened. The SV_{AVPD} is again indicated in grey and is identical to the grey regions in panels A and B. This illustrates that the area at d_1 (the largest short axis diameter) shall be used when calculating the SV_{AVPD}. The SV_{AVPD} would be underestimated if the area of either the mitral annulus at d_2 or the endocardial area at d_3 would be used. Panel D shows the grey region in A and C divided by a dotted line and broken apart. When adding them together, the grey region in B is generated. This illustrates why the largest epicardial area of the ventricle should be multiplied by the AVPD in the derived method for

calculating SV_{AVPD}.

Panel E shows a schematic short-axis view in end diastole (solid line) and end systole (broken line) at the level of the thin dotted line in C. The horizontal dashed lines indicate the position of the non-moving epicardium in end diastole and end systole. Note that in this model there is no radial sqeezing motion. However, the endocardium will still move inwards during systole as the result of the longitudinal AVPD, and this gives the false impression of a squeezing motion when the endocardium is viewed in a short-axis plane.

Panel F shows a heart in four-chamber long-axis MR images (panels 1 and 2) and corresponding short-axis images at the levels indicated by thin dotted lines (panels 3-6). The left ventricle (LV), right ventricle (RV), left atrium (LA) and right atrium (RA) can be seen. The solid white line is the contour of the epicardium in end diastole. The end-diastolic epicardial contour is copied to end systole. The curved dotted line in panels 1 and 2 is the basal contour of the epicardium in end diastole moved to the position of the AV-plane in end systole. The area between these contours (arrows) corresponds to the grey region in A-D. The piston-like movement of a smaller basal part of the ventricle into a larger midventricular part as seen in panels 1 and 2 explains most of the apparent epicardial movement inwards during systole seen in panels 3 and 4. In contrast, the epicardial area from the level of panels 5 and 6 becomes smaller as the position approaches the apex. At this level, the longitudinal AVPD will not move a smaller area into a larger area in the apical and midventricular parts of the ventricle. This means that the epicardial inward movement at these levels rather reflects true radial function.

The importance of using epicardial contours for these calculations can also be explained by the analogy of the tube of a telescope which can shorten and lengthen along its long-axis. The volume of the telescope decreases when the tube shortens and this would be the stroke volume of the tube. In order to calculate the stroke volume of the tube, two measures need to be known. 1) The decreased length of the tube (the AV-plane displacement of the LV), and, 2) the outer cross sectional area of the tube (the short axis epicardial area). The outer area of the tube would be used because the decrease in volume is not affected by what is inside the tube. The volume decrease is only affected by what has disappeared from where the tube was before it was shortened lengthwise. Two tubes with the same outer area but one with a thick wall and the other with a thin wall (different thickness of the myocardium in the LV) will decrease the same volume given the same outer area and same longitudinal shortening. Also, the wall of the tube is non-compressible, i.e. it retains its volume when shortening the tube. This analogy is true for the myocardium, the volume will be the same during the cardiac cycle because it is non-compressible.[69–71] The product of the AVPD and the short-axis area of the LV was found by Lundbäck to be in the same range

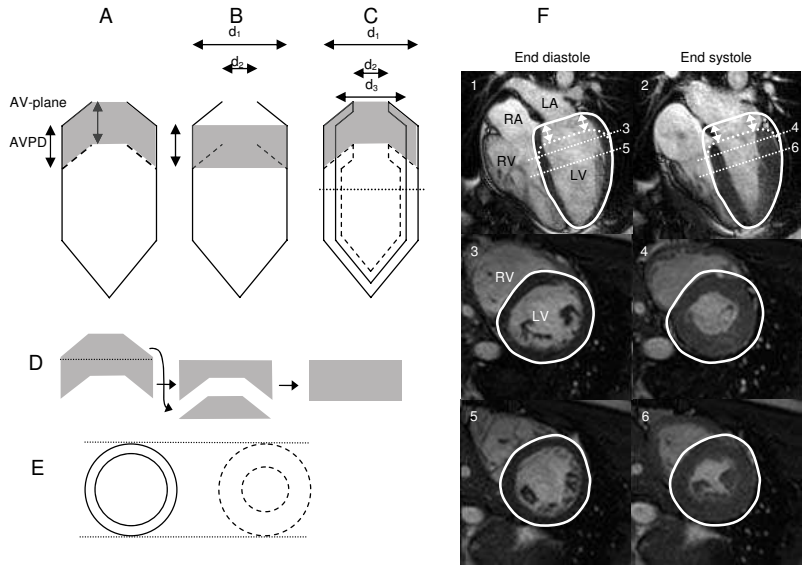

FIGURE 1.2 A schematic view of left ventricular pumping. See text for details.

as the reported normal LVSV from earlier studies.[42] Emilsson *et al.* used this equation with measurements obtained by echocardiography in healthy volunteers and found that approximately 80 % of the LVSV was generated by AVPD assessed by this method.[46]

Radial function is defined as the reduction in the epicardial short-axis radius of the ventricle caused by the squeezing of the ventricle. The endocardial movement towards the center of the lumen has previously been described as radial thickening due to the contraction of circular myocardial fibers.[9,72] However, the inward movement of the endocardium has been shown to be the result of more complex myocardial mechanics.[11,69,70,73,74] Isolated radial function is more difficult to assess because the inward motion of the endocardium is also the result of longitudinal shortening and redistribution of myocardium (Figure 1.2).[42,71,75] This can be understood by using the analogy of the tube of a telescope described above. The telescope has no radial function, the wall is made of a rigid non-compressible material. However, when the tube shortens along its long axis, the inner diameter of the telescope will diminish because the walls of the tube will accumulate within the shortened tube. This is an observed radial inward movement which in

reality is caused by longitudinal shortening. Therefore, the outer walls, i.e. the epicardium, must be studied when investigating isolated radial function.

Furthermore, the epicardial area at the mitral annulus in end diastole is smaller than the mid-ventricular area because of the dome shape of the basal part of the LV. As illustrated in Figure 1.2, the dome shape will contribute to an apparent inward epicardial motion at the base of the LV during AVPD. Isolated radial function can be identified in the radial inward movement of the epicardium in the midventricular and apical two-thirds of the LV.

The macroscopic perspective of radial and longitudinal function of the heart is relatively straightforward. However, coupling the volume changes of the cardiac chambers to the function of the different myocardial fiber layers is somewhat more complicated. The contractile unit of the myocardium is the sarcomere, and the sarcomere can shorten by 10-12 %.[59] A consequence of the different angles between the myocardial fibers and the ventricular wall is that contraction results in myocardial shortening in the longitudinal and radial direction as well as a torsion of the myocardium around its long axis.[8,9,14,15] The apical part of the left ventricle rotates around the long axis counter clockwise with respect to the base as viewed from the apex, whereas the basal part rotates in the opposite direction, i.e. clockwise. This has been proposed to be an effect of more epicardial than endocardial fibers, a greater radius in the epicardium giving a greater force, the delay of excitation of the epicardium and tethering or transmural mechanical coupling.[15] The torsion of the left ventricle results in a "wringing" of the left ventricle that has been studied by implanted radiopaque markers[15,76,77] and MRI.[78,79] Detailed information about myocardial contraction can also be obtained non-invasively by Doppler[80–82] or MRI measurements[83,84] of myocardial velocities during the cardiac cycle to quantify regional function. However, this thesis did not seek to investigate the intrinsic mechanics of the myocardium but rather the volume changes of the total heart and individual chambers, and therefore myocardial torsion or regional myocardial function has not been studied.

Outer volume variations in relation to the longitudinal and radial function of the ventricles

As discussed above, a relationship between longitudinal function and the relative constancy of the heart has been proposed. However, the quantitative relationship between outer volume variations and the function of the ventricles has not been studied. Figure 1.3 presents five theoretical models (A-E) of the outer volume variations of the heart in relation to longitudinal and radial function of the ventricles and atrial filling. For simplicity the model includes the epicardial borders of a single atria and a single ventricle, and the inflow from the veins is shown at the top and outflow to the arteries at the bottom. The volume of the myocardium

is constant over the cardiac cycle[69–71, 85] and is thus omitted from the model for simplicity. The piston-like atrioventricular plane displacement (AVPD) is indicated by double-headed arrows. Solid lines indicate the end diastolic position and dotted lines the positions in end systole. The total stroke volume (TSV) of the ventricles is generated by longitudinal (SV_{long}) and radial (SV_{rad}) function. SV_{long} is generated by AVPD and SV_{rad} by inward displacement of the outer walls of the ventricle. Model A has no radial function of the ventricles, instead the AVPD generates the entire stroke volume and the simultaneous atrial filling. Thus, there is no total heart volume variation (THVV) and no center of volume variation (COVV). In model B, the TSV is generated by a combination of radial and longitudinal function. Atrial filling is coupled to the longitudinal function and thus THVV will be identical to SV_{rad}. There will be a small COVV in the direction of the base of the heart because of the radial diminishment of the ventricles and the constant atrial diameter. Model C illustrates a situation with no AVPD and thus no longitudinal function. The TSV will be identical to SV_{rad}. Atrial filling during systole in spite of no AVPD causes the atria to expand radially while the ventricles diminish. This will lower the THVV, but the COVV will be high. In model D, AVPD generates the TSV as in model A, but atrial filling is zero. Thus, the outer walls of the atria will move inwards. THVV will be equal to SV_{long} and the COVV will be high. Model E shows a combination of SV_{long} and SV_{rad} as in B but SV_{long} is larger and atrial filling is slightly less than SV_{long}. This will result in a larger THVV than SV_{rad} but a lower COVV compared to model B. In conclusion, both THVV, COVV and either radial or longitudinal function must be determined to quantitatively determine the relationship between outer volume variations and function of the ventricles.

1.2 Magnetic Resonance Imaging

Theoretical background

All protons and neutrons have a small magnetic field due to the quantum mechanical property of "spin". The hydrogen nucleus consists of a single proton. The hydrogen nuclei that give MR signal are mainly bound in water molecules, but also hydrogen in fat and other molecules contribute. When a body is placed in a magnetic field two things happen to its spin. The small magnetic field of the body will align either along the external field or against it. There is a small surplus of spins along the field compared to against the field and that will result in a small net magnetization vector, called M. The M vector determines the maximum MR signal that can be measured. Furthermore, the spin will rotate around an axis parallel to the magnetic field, this motion is called precession. The frequency of the precession is called the Larmore frequency and is directly proportional to the

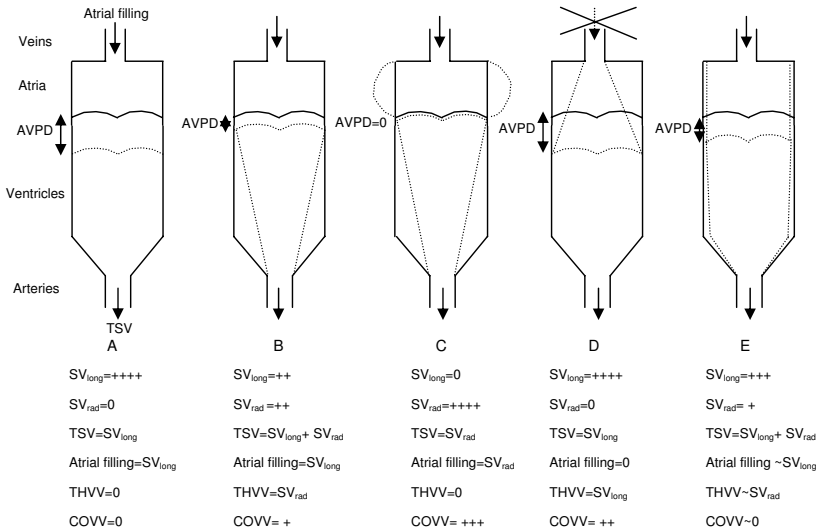

FIGURE 1.3 Five theoretical explanations for different total heart volume variations. For details see text.

magnetic field. The Larmore frequency for hydrogen nuclei is 42.6 MHz/T. The spin can be affected by energies sent into the system at the Larmore frequency, as this is the resonance frequency of the system. The absorbed energy will alter the direction of the vector M. If the direction of M is changed from along the field it can be detected, as it is no longer hidden by the much larger surrounding magnetic field. The component of M that is perpendicular to the main field will rotate around the direction of the main field with an angular velocity equal to the Larmor frequency. An antenna can detect this rotating component. This rotating component can be viewed as an echo of the energy sent into the system. The signal obtained from the body is sampled in the frequency domain or k-space, and is reconstructed by Fourier analysis to provide the image.

The amount of energy needed to change the vector M to an orientation perpendicular to the magnetic field is called a 90° pulse. After this energy has been deployed the vector M will start to return to its origin. This is called relaxation and occurs in two ways: 1) a gradual increase in the magnitude of the M vector along the magnetic field (described by the time constant T1) and 2) dephasing or splitting of the vector M perpendicular to the magnetic field (described by the time constant T2). Different tissues have different T1 and T2 values, and this is used for creating contrast between tissues in the image.

The MRI scanner is composed of several coils. One coil creates a large magnetic field, in modern scanners typically 1-3 T. In comparison, the magnetic field of the earth is 30-60 μT. The large magnetic field in the MR scanner is maintained by the superconducting wiring. In a superconducting wire, the temperature of the metal is lowered by liquid helium to a temperature near the absolute freezing point and this eliminates friction and enables large currents to be used without energy loss. Thus, the magnetic field of the MRI scanner is always on, and turning it off is a complicated process that takes time, effort and is expensive. Three gradient coils are used for inducing small variations in the magnetic field that are used to select the imaging plane. Surface coils are receiver antennae that are used close to the body as to increase the sensitivity for detection of signals from the body. The programs used for directing the currents in the coils are called sequences and different sequence parameters are used to provide different images. MRI is sensitive to motion and physiological triggering is needed when imaging the heart. The motion of the heart is corrected for by cardiac triggering and respiratory motion is minimized by imaging during breath hold. Cardiac triggering is most often performed by prospective or retrospective ECG triggering. In prospective ECG triggering, the MR scanner automatically detects the R-wave and image acquisition begins at that point and continues for a determined length of time. The RR interval determines the length of time available for image acquisition but often the last part of the cardiac cycle, the atrial contraction, is not imaged. Modern scanners are able to use retrospective triggering which gives the ability to image the complete cardiac cycle. This is done by continuous image acquisition and parallel detection of the ECG. After image acquisition, the images are arranged in the appropriate part of the RR interval. Pulse triggering can be used if the ECG signal is not optimal. Fast imaging techniques make it possible to acquire images in real time, thereby making triggering unnecessary. However, the real time images have lower spatial and temporal resolution.

Cine imaging and volume measurements

Volume measurements in studies of heart function are often performed using two-dimensional techniques and geometrical assumptions of heart shape.[86–88] An example is the Simpson's biplane formula often used in echocardiography.[21] All two-dimensional techniques will be limited by these geometrical assumptions.[89] MRI gives the opportunity to image the body using parallel image planes (Figure 1.4). The volume of each slice is obtained by delineation of the borders of the heart and multiplying the area by the slice thickness. The volume of the body is obtained by adding the delineated volumes of all slices. Volume measurements by MRI have been shown to be reliable, accurate and have low interobserver variability.[90] This has made MRI the gold standard for assessing the cavitary and

myocardial volumes of the heart.[91–99] Reference values for cardiac volumes in humans by MRI are now available.[30, 100, 101]

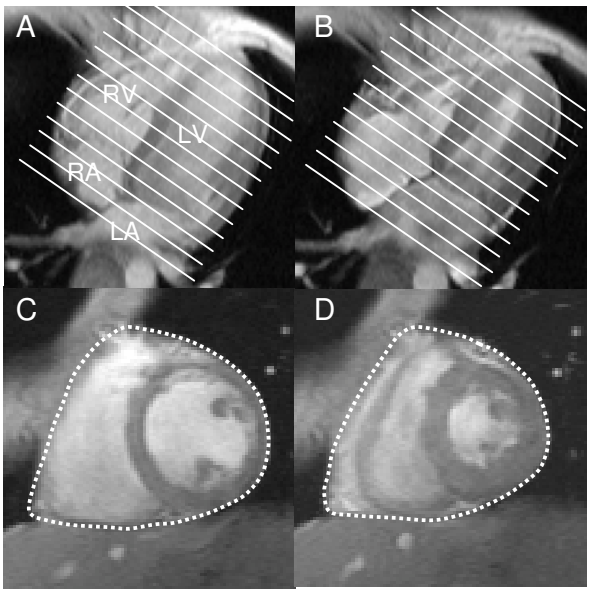

FIGURE 1.4 Measurement of cardiac volumes by MRI. The top panels show long-axis views of the heart in end diastole (A) and end systole (B). The heart is imaged from apex to base in the short axis view (bottom panels) as indicated by white lines in A and B. The dotted lines in the bottom panels indicate the pericardial borders of the heart in end diastole (C) and end systole (D). The volumes of all slices are added to obtain the entire volume of the heart.

Flow imaging and analysis

MRI provides the opportunity for non-invasive flow measurements with excellent accuracy and precision in large vessels[102–111] and even vessels at the size of the coronary arteries.[112–114] Also, MRI flow quantification has been shown to be equally accurate and less variable compared to both Fick principle[115] and thermodilution.[116] This is performed by measuring the velocity of the tissue in the direction perpendicular to the imaging plane by phase velocity mapping.[117] The

velocity of all tissue is measured and the velocity of the flow in the vessel is used for analysis. In short, magnetic field gradients are used to encode the velocity into an image. The precession frequency will change in an object moving in a varying magnetic field. This will affect the phase angle in a linear relationship to the velocity of the object. A phase image can be reconstructed that depicts the phase angle information in proportion to the grey scale value of the image. The signal intensity can be measured in each pixel of the image and will be directly proportional to the velocity of the tissue in that pixel. Thus, the phase image can be used as a velocity map of the tissue. In theory the phase or velocity of non-moving tissue, e.g. chest wall, will be zero. Unfortunately, there can be disturbing factors such as eddy currents and inhomogeneities of the magnetic field that will alter the velocity information. Therefore, it is of importance to perform in vitro and in vivo calibrations of each MRI scanner. In addition, filters and background corrections can be used. Flow imaging also generates anatomic (or modulus) images that can be used for identification and delineation of the vessel whereas the phase images contain corresponding information about flow velocity.

Figure 1.5 shows an example of the velocity mapping technique with modulus and phase images in the inferior caval vein. The grayscale values of each pixel in the phase images are directly proportional to velocity. Thus, within a region of interest (ROI), the average blood flow velocity for any given time point throughout the cardiac cycle can be calculated while the cross sectional area of that vessel is simultaneously measured. This allows for calculation of absolute blood flow at each time point by the following equation:

$$\text{Average Velocity} \times \text{Area} = \text{Average Flow}$$

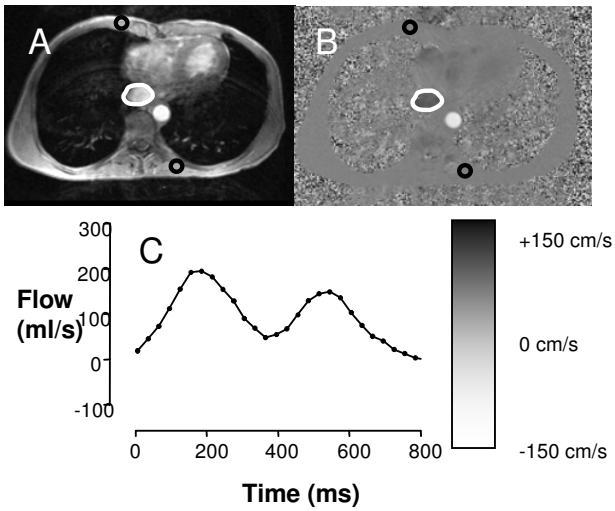

FIGURE 1.5 Phase velocity mapping of the flow in the inferior caval vein encircled in white. Black circles indicate ROIs used for background correction.

Chapter 2

Aims

The general aim of this thesis was to examine new aspects on human cardiac pumping which may help to understand pumping physiology and pathophysiology MRI.

The specific aims for each paper were:

I. To investigate the magnitude and timing of the total heart volume variation (THVV) during the cardiac cycle in healthy adults.

II. To determine the direction and extent of the center of volume variation (COVV) throughout the cardiac cycle in healthy adults and assess THVV and COVV in patients with cardiac failure due to ischemic heart disease before and after cardiac surgery.

III. To measure the percentage of the left ventricular stroke volume explained by AV-plane displacement (SV_{AVPD}) in healthy subjects, athletes and patients with severely decreased left ventricular function due to dilated cardiomyopathy (DCM).

IV. To determine if the SV generated by radial contraction is equal to the outer volume variations of the left, right and total heart. Also, to meausure the SV_{AVPD} of the right ventricle.

V. To quantify the increase in total heart volume which occurs before the end of systolic ejection and to quantify the decrease in THV caused by the outflow from the heart through the veins during atrial contraction.

Chapter 3

Materials and Methods

3.1 MRI scanners and sequences

MRI scanners

In study I and II a 1.5 T Magnetom Vision (Siemens, Erlangen, Germany) with 25 mT/m maximum gradient strength was used to acquire all images. In study III, IV and V a 1.5 T Philips Intera CV (Philips, Best, the Netherlands) with 33 mT/m maximum gradient strength and a cardiac synergy coil was used.

MRI sequences

Cine imaging

Siemens: Prospective ECG-triggered gradient-echo sequences were used to obtain cine images during end-expiratory apnea (approximately 15 seconds). The number of phases was determined by the RR-interval resulting in 15-21 images per heart cycle. Typical imaging parameters were, repetition time 100 ms with echo sharing resulting in one phase every 50 ms, echo time 4.8 ms, flip angle 30°, slice thickness 10 mm and no slice gap.

Philips: A steady-state free-precession sequence with retrospective ECG triggering was used to achieve 30 phases per cardiac cycle and giving a temporal resolution of typically 30 ms, repetition time 2.8 ms, echo time 1.4 ms, flip angle 60°, spatial resolution of 1.4x1.4, slice thickness 8 mm and no slice gap. Parallel imaging with a SENSE factor of 2 was used in the short-axis images.

Flow imaging

Siemens: A free breathing gradient-echo velocity mapping sequence with prospective ECG triggering provided by the manufacturer was used. Typical

imaging parameters were: repetition time 30 ms, echo time 5 ms, slice thickness 8 mm, VENC of 150 cm/s for arteries and 80 cm/s for veins. In the case of aliasing the study was repeated with a higher VENC. Velocity information was acquired over one or two heart cycles and the acquisition time was 3-7 minutes. Background correction was performed manually to correct for field inhomogenities. Two regions of interests (ROI) were drawn in stationary tissue at approximately equal lengths from the vessel investigated, as previously described.[103] The average signal intensity of these ROI:s in non-moving tissue were set to represent zero cm/s.

Philips: An in-house adapted, free breathing fast field echo velocity encoded sequence with retrospective ECG triggering was used to obtain full coverage of the cardiac cycle. Typical imaging parameters were: repetition time 10 ms, echo time 5 ms, flip angle 15°, slice thickness 6 mm, 35 phases, number of acquisitions 1, no parallel imaging and a VENC of 200 cm/s for arteries and 80 cm/s for veins. The in-plane spatial resolution was typically 1.2x1.2 mm and the temporal resolution was dependent on the heart rate. If suboptimal image quality was found in the free breathing images, flow measurements were performed using a breath hold turbo field echo velocity encoded sequence with retrospective ECG triggering. Typical imaging parameters of the breath hold flow sequence were: repetition time 4.5 ms, echo time 2.9 ms, flip angle 15°, slice thickness 10 mm, 40 phases, number of acquisitions 1, SENSE factor of 2, an in-plane spatial resolution of 1.2x1.2 mm. A linear phase correction filter supplied by the manufacturer was used for background correction.

3.2 Study population

In study I, eight healthy volunteers were examined by cine and flow MRI to obtain total heart volume variation over the cardiac cycle. The subjects were 26-47 years old and five were males. The volunteers declared that they were healthy and had no prescribed cardioactive drugs, blood pressure was below 140/90 and ECG was normal. The images from six of these volunteers were used in study II to acquire center of volume information, namely the subjects 1, 2, 3, 4, 7 and 8 listed in table 1 of study I. The remaining two subjects were not used because the data from the first six subjects analyzed was consistent and thus were sufficient. Center of volume variation and total heart volume variation was also measured in eight patients before and after cardiac surgery. They were enrolled in a trial designed to study changes in cardiac function after coronary bypass surgery in patients with depressed cardiac function.[118] The patients were 56-74 years old, all men, were scheduled for first time coronary bypass surgery and had ejection fraction below 50 % as determined by echocardiography. The MR examinations were performed

the week before and approximately one month after surgery. Coronary bypass surgery was performed with grafting of the left anterior mammary artery and 0-4 venous grafts, and the pericardium was not closed, but opposed by a few stitches. In study III, 12 healthy subjects (mean age 24 years, 5 women) were imaged for comparison with 12 triathletes (mean age 35 years, 4 women) and 12 patients (mean age 54 years, 4 women) with dilated cardiomyopathy. The 12 healthy subjects were imaged by cine images covering the short axis and the three long-axis as well as flow images of all vessels to and from the heart. The triathletes and patients were imaged by cine images similar to the control subject, but flow images of all vessels to and from the heart were not acquired. The triathletes were imaged as a part of a study of heart function in athletes using ergospirometry and cardiac MRI. Patients were imaged in clinical routine and enrolled after reviewing the charts for patients with dilated cardiomyopathy who had ejection fraction below 30 %. Patients with ischemic genesis to the dilated cardiomyopathy were not included. Of the 12 healthy subjects in study III, 11 could be used for the subsequent studies IV and V. The remaining subject could not be used because of aliasing and misplaced flow planes resulting in suboptimal flow images. The subjects are given the same number in study IV and V.

3.3 Total heart volume variation

The total heart volume (THV) was defined as the volume of all structures within the pericardium, including myocardium and blood of both ventricles and atria and pericardial fluid. The pericardium covers the proximal parts of the great vessels and thus these parts were included in the measurements. A region of interest was manually drawn around the pericardial borders of the heart of all slices covering the heart from apex to the base of the heart of all images throughout the cardiac cycle (studies I and II) or only in end diastole and end systole (study IV). The total heart volume in end diastole was used as reference value for calculations of total heart volume variation (THVV). The myocardium and pericardial fluid is non compressible and thus remains constants during the cardiac cycle. Blood in the chambers is the only volume within the pericardium that varies over the cardiac cycle. The blood volume in the coronary vessels will not cause an error as they originate and empty within the pericardium. Hence, THVV measures the difference in blood leaving the heart and entering the heart. A new method for calculating THVV by flow imaging was developed. Flow images of all vessels leading to the heart (caval and pulmonary veins) and from the heart (the aorta and pulmonary trunk) were obtained. Adding all inflow (ml/s) into the heart and multiplying by time (s) gives the increase in THV (ml) for each time point. Likewise, adding all outflow from the heart gives the decrease in THV for all

time points. Total heart volume variation can then be calculated by subtracting the decrease of THV from the increase in THV. Flow imaging gives the absolute changes in THV and to get the relative changes in THV, the THVV by flow was divided by the THV at end diastole obtained from the cine images.

3.4 Center of volume

Calculations of the center of volume variation (COVV) were used for the total heart in study II and for the left and right ventricle in study IV. The center of volume is the geometrical center of a body and can be calculated by dividing the volume in a series of parallel images covering the volume. By weighting the coordinates ($Coordinate_1$ to $Coordinate_n$) for each slice by the volume of that slice (Vol_1 to Vol_n) the coordinate for the center of volume can be calculated using equation 1 in study II. The center of volume has three coordinates and the calculation is performed for each coordinate individually. The calculations were done for all time frames during the cardiac cycle in study II and for the end diastolic and end systolic images in study IV. The maximum distance between the coordinates was calculated using equation 2 in study II.

3.5 Atrioventricular plane displacement

Atrioventricular plane displacement (AVPD) was measured in studies II, III and IV. AVPD was defined as the distance between the AV-plane from end diastole to end systole perpendicular to the AV-plane position in end-diastole. AVPD of the left ventricle was measured at the basal part of the muscular wall in three long-axis images resulting in six measuring points placed 60 degrees apart in a short axis view (Figure 3.1). The position of the most basal point of the left ventricular myocardium was manually traced and the mean of the motion was used for calculations. Apical motion was calculated in the same images and along the long axis of the ventricle and the mean distance of the three images was calculated. AVPD of the right ventricle was calculated from two of the three long axis views, namely the four-chamber and left-ventricular outflow-tract view. The basal point of the right ventricular myocardium of the free lateral wall was manually traced in the four-chamber images and the basal point of the right ventricular outflow tract was manually traced in the left-ventricular outflow-tract images. The interventricular septum is part of both ventricles and has lower AVPD than the free wall of the RV. The mean septal motion was calculated from the four-chamber and left-ventricular outflow-tract images. AVPD of the RV was calculated as the mean of the septal motion and the motion of the free wall and right ventricular outflow tract.

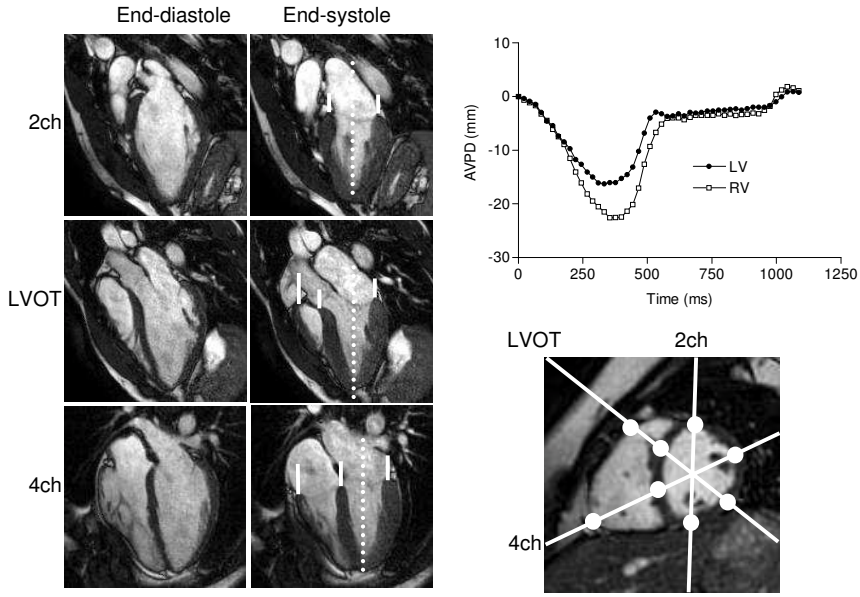

FIGURE 3.1 The measurement of AVPD in three long axis images (left), the AVPD over the cardiac cycle for the LV and RV (top right) and the position of the measurement points for AVPD (white dots) shown in a short axis image (bottom right). AVPD was measured perpendicular to the AV-plane at end diastole as indicated by vertical white dotted lines. The AVPD is shown by white solid lines.

3.6 Longitudinal function

Longitudinal function was defined as the portion of the stroke volume generated by AVPD (SV_{AVPD}). The proposed method[42] of multiplying the AVPD by the LV epicardial area does not take into account the varying short-axis area of the part of the LV encompassed by the range of the AVPD. Therefore, we further developed the method proposed by Lundbäck by using the mean of the largest short-axis areas encompassed by the AVPD (Figure 1.2). To validate this derived method, longitudinal function was also measured by direct volumetry in a stack of radial long axis slices.[119, 120] For each long-axis slice in a radial stack, the epicardial border of the LV in end diastole was outlined and the position of the AV-plane in end systole was identified. The outline of the epicardial border of the LV in

end diastole was translated along the long-axis of the LV towards the apex so that the basal part of the outline had a position corresponding to the position of the AV-plane in end systole. The volume difference between the two borders in the base of the end diastolic contour was calculated for all radial slices.

No method for calculating the SV_{AVPD} of the right ventricle has previously been proposed. In study IV, the same method as for the LV was used to calculate SV_{AVPD} of the RV. However, the validation of the method in the long axis views is more complicated because of the complex anatomy of the RV. Therefore, we performed the direct volumetry of the SV_{AVPD} between the AV-plane in diastole and systole in images obtained by multiplanar reconstruction from the short axis images. This enabled the visualization of the contours of the RV in perpendicular long axis views in systole and diastole. Stroke volume for the LV and RV was calculated as previously described.[121, 122]

3.7 Integration of outer and inner volume changes of the heart

Atrial filling is coupled to ventricular ejection by AVPD, and the relative constancy of the THV is explained by an inner volume displacement within the heart caused by the longitudinal shortening of the ventricles (AVPD).[41–43] The remaining radial function of the ventricles or radial squeezing of the LV is not caused by AVPD, and thus not related to atrial filling during systole. Therefore, the outer total heart volume variation (THVV) is related to radial function.[123] THVV determined by flow imaging was compared to radial function calculated as the stroke volume minus the volume attributed to longitudinal function. This was performed for each ventricle individually using flow measurements in the vessels to and from the corresponding part of the heart, and for the total heart using all flow to and from the heart as described above.

3.8 Late ejection filling volume

The late ejection filling volume (LEFV) was defined as the increase in THV which occurred between minimum THV and the end of systolic ejection as calculated from the flow data. Figure 3.2 shows flow and cine data from one typical subject. Panel A shows the atrioventricular plane displacement (AVPD) of the left ventricle (LV) and the right ventricle (RV). Panel B shows the total heart volume (THV) and volume of the LV and RV. Note that the THV in the latter part of diastole is greater that the THV in end diastole. Panel C shows flow in the pulmonary trunk and the combined flow of the inferior and superior caval veins. Panel D shows flow in the aorta and the combined flow of the pulmonary veins. Panel E shows

the sum of the outflow (aorta and pulmonary trunk) from and inflow (caval and pulmonary veins) to the heart. Line 1 indicates when inflow to the heart exceeds the outflow during late systole which corresponds to the time of the lowest THV seen in B. Line 2 indicates the end of systolic ejection. The area between lines 1 and 2, indicated by diagonal lines in E represents the late ejection filling volume (LEFV). Minimum THV will occur when outflow is equal to inflow in the later part of systole. Thereafter, inflow is greater than outflow and THV will increase. The end of systolic ejection was defined as when the combined systolic flow of the aorta and pulmonary trunk reached 0 ml/s. The magnitude of the LEFV was expressed in absolute volume as well as percent of both THV and THVV. Also, the LEFV was compared to the total stroke volume and the rate of systolic AVPD. Furthermore, the LEFV was quantified separately for each side of the heart as the flow difference between the lowest heart volume and end of systolic ejection for the left and right side of the heart, respectively.

3.9 Atrial wave reversal volume

The atrial wave reversal volume (AWRV) was defined as the volume of blood exiting the heart during late diastole through the veins. Figure 3.2 shows a negative flow at the end of diastole in all veins, coinciding with atrial contraction as seen in A, and resulting in the decrease of the THV in late diastole as seen in B. The AWRV was measured as the negative flow seen in the veins during late diastole multiplied by time from the beginning of the late diastolic negative flow until end diastole. The AWRV was measured for the left, right and total heart, respectively. The total heart AWRV was also expressed as percent of both THV and THVV.

3.10 Image analysis software

In study I and II, Scion Image (Scion Image, Scion Corporation, Maryland, USA) was used for flow and volumetric measurements. In study II atrioventricular plane movement measurements was performed using the freely available software ImageJ v.1.32j (http://rsb.info.nih.gov/ij/). For flow analysis in study I, RADGOP (Context Vision, Linköping, Sweden) was used by the second observer. In studies III-V the freely available software Segment was used (Segment 1.4-1.6, http://segment.heiberg.se).[124]

3.11 Statistical analysis

Continuous variables are expressed as mean ± standard error of the mean (SEM) and the range. The non-parametric Mann-Whitney test was used to determine

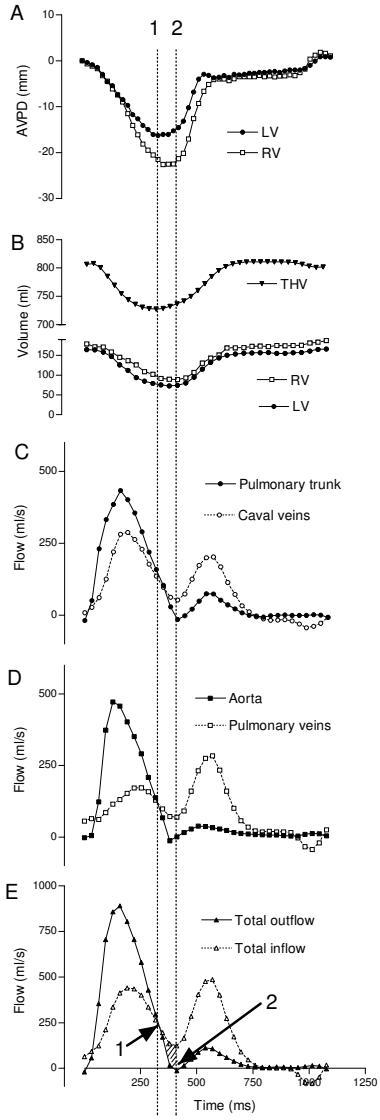

FIGURE 3.2 AVPD, cardiac volumes and flow over the cardiac cycle from one typical subject. See text for details.

the significance of the differences between variables. The non-parametric Wilcoxson test was used in study II to determine if variables were different before and after surgery. In study I the inter-observer variability or method concordance was calculated using the intraclass correlation coefficient (ICC).[125] Bland-Altman analysis[126] was used to test if two methods used to measure the same parameter differed. In study I, the paired t-test was used to test if the changes in apex-base length were significant. A p-value <0.05 was defined as statistically significant. The relationship between variables was determined by Pearson's correlation coefficient.

Chapter 4

Results and Comments

4.1 Total heart volume variation

Studies I, II, IV and V

Although variations in total heart volume affect cardiac efficiency, little is known about the variations in total heart volume in humans. Therefore, in study I the total heart volume variation (THVV) was determined in eight healthy volunteers. The study used two independent methods of determining THVV during a cardiac cycle, namely, volumetric and flow imaging. The volumetric and flow methods showed similar results, 8.2±0.8 % (range 4.8-10.6 %) vs. 8.8±1.0 % (range 5.6-11.8 %). ICC of the two methods was 0.999 and the difference between the volumetric and flow method according to Bland-Altman analysis was -0.6%±1.0 % (SD). The concordance of the findings by the two methods both in magnitude and time course in all subjects implies that the range of the total heart volume variation between subjects likely demonstrates a true physiological variation (Figure 4.1). The inter-individual variation of THVV between healthy subjects has not been described previously. The physiological significance and the cause of the variation between healthy subjects were still unclear at this point and therefore further studies of THVV were undertaken.

The constancy of THV over the cardiac cycle has been proposed to be dependent on AVPD[41–43,45,57] and therefore we compared THVV in patients with decreased AVPD with healthy volunteers in study II. The AVPD differed between healthy volunteers (16.3 ± 0.7 mm) and patients before surgery (9.9 ± 0.6 mm, p = 0.002) and after surgery (10.2 ± 0.5 mm, p = 0.002). Patients after surgery did not differ in AVPD compared to before surgery (p = 0.40). Although the patient population had a lower AVPD, THVV before surgery (6.9±0.2 %, range 5.1-9.3

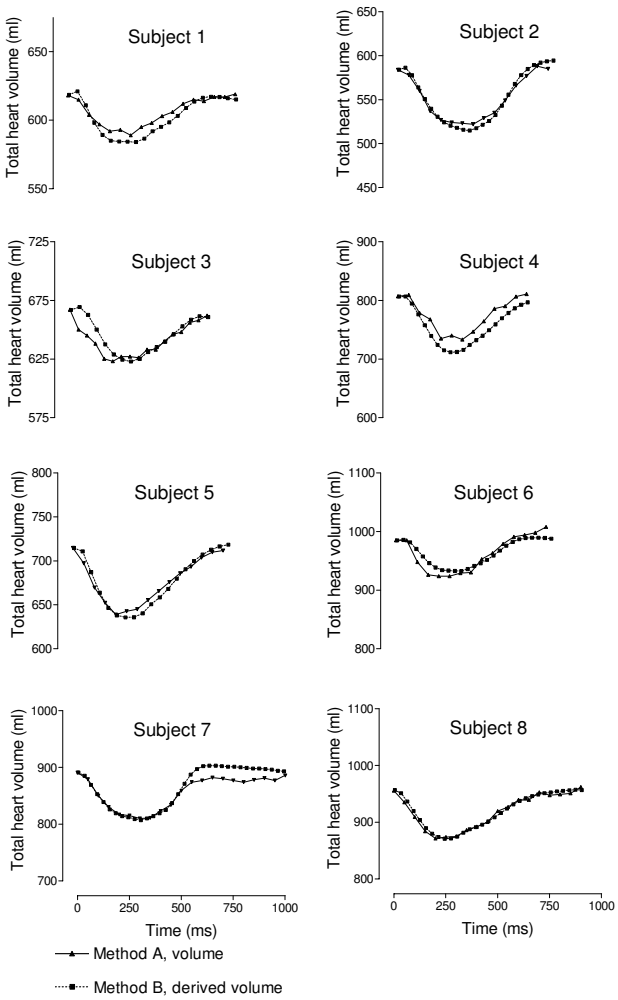

FIGURE 4.1 The THV throughout the cardiac cycle in all subjects of study I by volumetric (volume) and flow (derived volume) imaging.

%) and after surgery (7.5±0.2 %, range 5.8-9.5 %) was not significantly larger compared to the healthy subjects (7.3±0.4 %, range 4.0-9.1), (p=0.61 and p= 0.80 respectively). Thus, study II, found no difference in THVV when comparing healthy subjects and patients with decreased ejection fraction and significantly reduced AVPD. This suggests that the THVV cannot be explained only by the magnitude of AVPD.

The relationship between THVV and the relationship between radial and longitudinal function of the ventricles was further investigated in study IV, see section 4.5. THVV has been proposed to be dependent on the pericardium,[49] but earlier studies have suggested minimal pericardial influence on the constant THV.[127, 128] Therefore, the THVV before and after pericardiotomy (bypass surgery) was compared to elucidate the effect of the pericardium on the constant THV. A statistical significance was found (p=0.05) between THVV after surgery (7.5±0.2 %, range 5.8-9.5 %) compared to before surgery (6.9±0.2 %, range 5.1-9.3 %). However, the magnitude of the difference was very low and visual assessment of the time-volume curves shows that the THVV was nearly unchanged by the coronary-bypass surgery, and that the time course of the change in THV was essentially similar in all subjects (Figure 4.2). The THV decreased in the majority of patients, but notably the relative THVV was not affected. This may indicate that the THVV (magnitude and time course) is a physiological parameter different from patient to patient, but constant over time, even after interventions such as cardiac surgery.

The explanation for no apparent increase in THVV after surgery despite pericardiotomy may be that structures other than the pericardium around the heart (thoracic wall, liver, lung and mediastinum) play an important role in the constraint of the heart[129–131] and thus could be responsible for maintaining intracycle relative constancy of THV. The pericardium was, however, loosely opposed by stitches according to standard surgical procedure, which could mean that the pericardium may retain some of its function. The measurements of THVV by cine and flow imaging were repeated in a new population of healthy volunteers in another MRI scanner in study IV. The THVV of healthy subjects in study IV (8.4±0.6 %, range 5.7-11.1 %) was similar to study I (8.2±0.8 %, range 4.8-10.6 %). The volumetric and flow method showed similar results also in study IV (r=0.95, p<0.001) and bias was low (4.0±7.8 ml). This gives further evidence of the physiological explanation for the range of THVV between subjects. For further discussion on the explanation of THVV see section 4.5.

Cine images were used to find the anatomical location of the outer volume changes during the cardiac cycle (study I). The major contributor to the volume change is the region around the AV-plane displacement. For any given cardiac MRI short-axis imaging plane, the change in volume was essentially proportional to the starting volume in that plane (R^2 = 0.43). The predominant volume

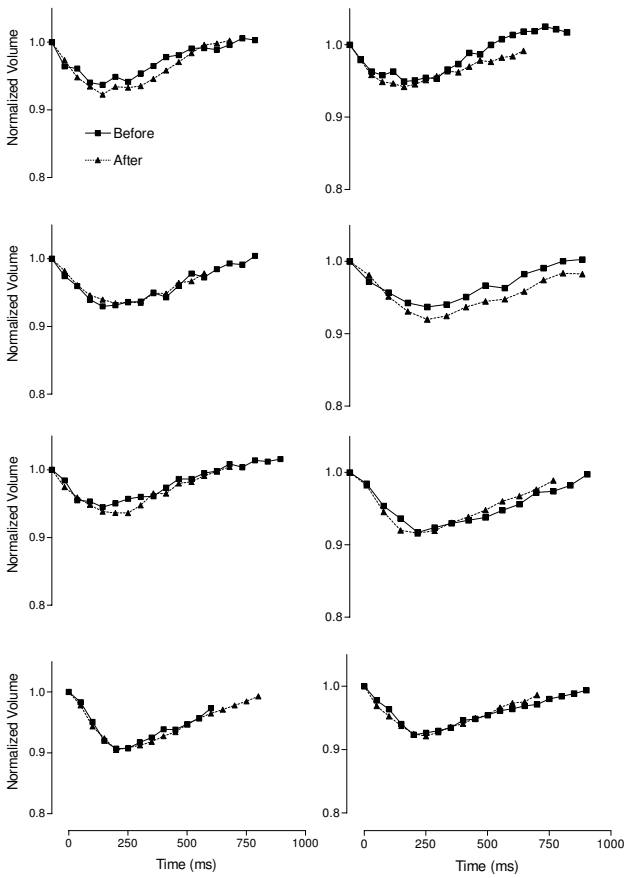

FIGURE 4.2 The THV throughout the cardiac cycle normalized to the THV at end diastole before and after cardiac surgery for all patients of study II.

changes were visually observed where the heart was most adjacent to the lungs while the regional changes in volume at the borders to the liver were less and were essentially absent near the thoracic wall (Figure 1.4 and Figure 4.10).

The contributors to THVV can also be studied using the flow patterns in and out of the heart. The left side of the heart contributed to a majority of the THVV (61±2 %, range 52-70 %). The outflow showed a pulsatile pattern in systole and the inflow was more continuous, and slightly biphasic with increases in flow both in diastole and systole (Figure 3.2 and Figure 4.3). In systole, outflow was greater than inflow (decrease in cardiac size) while the reverse was true during diastole (Figure 3.2 and Figure 4.3). This means that the proportion of blood ejected during systole exceeded the filling of the atria during systole, 24±1 % vs. 15%±1 % of the total heart volume (p=0.001). During systole 62±2 % of the stroke volume from the ventricles was secured by filling of the atria. This causes a decrease in total heart volume in systole due to a discrepancy in blood flow into and out of the heart with no significant longitudinal shortening of the heart during this process. The caval veins exhibit a flow pattern which is more similar to that seen in the great arteries compared to the flow patterns in the pulmonary veins. This flow pattern in the caval veins has previously been associated with normal right heart hemodynamics.[132] In study I, 64 % of the stroke volumes from both chambers were secured into the atria during systole (reservoir function of both atria). The reservoir function of the left atrium in percent of the stroke volume of the left ventricle has previously been reported to be 38 % as assessed by Doppler echocardiography[26] and 41 % as assessed by MRI.[133] Thus the reservoir function of the right atrium is higher than the left atrium. This can be visualized in the flow curves as a more bipolar flow in the caval veins with the highest peak in systole and a more continuous flow in the pulmonary veins. A similar biphasic pattern of blood flow during systole and diastole into the heart as in the present study, has been found in Doppler examination of caval and pulmonary veins.[40, 134]

Venous filling into the heart has been found to alter with heart rate.[36, 135] Proportionally greater systolic atrial filling over diastolic flow occurs at increased heart rates, compared to lower heart rates. At higher heart rates and cardiac output the momentum of the blood created by the descent of the AV-plane can thus be used for a more rapid filling of the expanding atria. This will cause less outer volume changes in the surrounding tissue, which would conserve energy. In addition, higher heart rates may result in a lower total heart volume change because of a shortened diastolic phase, and this possibly could make the outflow less pulsatile, and hence synchronize the in- and outflow.[42] This will result in a lesser total heart volume change at higher frequencies and is in line with the findings of Brecher,[136] Nilsson et al[137] and the conclusions of Gauer[45] that faster and smaller hearts secure 80 % of their stroke volume during ventricular systole. AVPD is also known to increase during exercise[36, 138, 139] and this may imply an increased

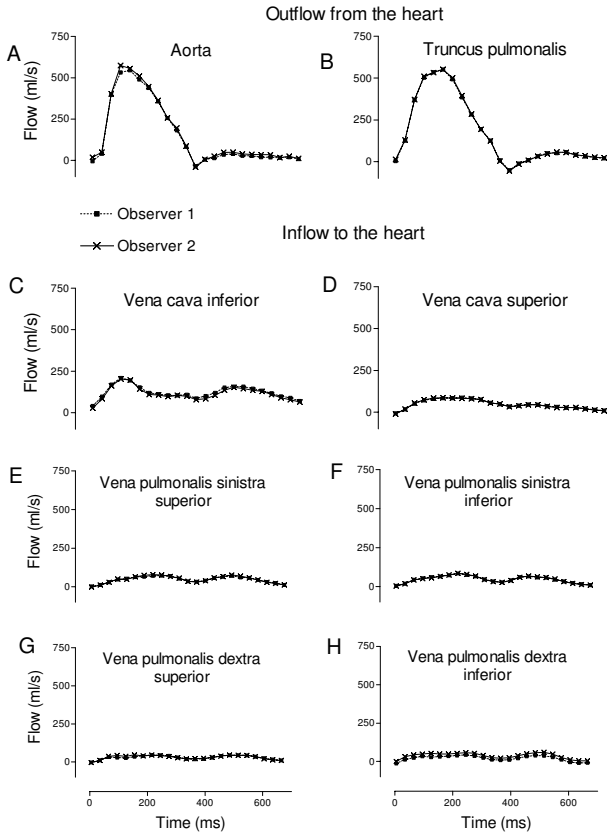

FIGURE 4.3 The results from two independent observers of all outflows from and inflows to the heart in one subject.

atrioventricular coupling in humans at higher heart rates.[36]

4.2 Center of volume

Studies II and IV

Work is defined as the product of mass, acceleration and distance traveled. Therefore, the mass of the heart, its acceleration and its distance traveled during the cardiac cycle all have implications for the energy expenditure and the efficiency of cardiac pumping. Therefore, the center of volume variation (COVV) for the total heart was calculated in Study II to measure the distance traveled by the heart during the cardiac cycle. In Study II the COVV in healthy subjects was 2.3±0.1 mm. The COVV was not significantly different in the patient population before surgery, 1.9±0.05 mm (p=0.09), Figure 4.4. After cardiac bypass surgery the COVV increased significantly to 3.6±0.09 mm (p=0.01), and this was significantly larger than in healthy subjects (p=0.007), Figure 4.4.

The COVV described a loop in all three dimensions that began and ended near each other, suggesting that this is a physiological finding and not random movement (Figure 4.5). After cardiac surgery the COVV doubled and the main direction of the loop was similar to that before surgery with the main movement being towards the right side of the heart in systole and back again in diastole. The pathophysiological significance of this is unclear but the constancy of the COVV has been proposed to influence the energy state of the heart, possibly influencing long-term pumping efficiency.[57] The explanation of the increased COVV after pericardiotomy could reflect the paradoxical movement of the interventricular septum towards the right ventricle.[140] The cause of this paradoxical septal movement is not fully understood and several explanations have been proposed, for example exaggerated cardiac mobility explained by the lack of restraint of the pericardium,[141] events during cardiopulmonary bypass,[142] systolic translation of the ventricle,[143] impaired motion pattern of the RV[144] and the displacement of septum at diastole because of a transseptal pressure gradient.[145] In the present study the largest COVV occurred in a direction similar to the paradoxical movement of the septum (see study II, figure 5). Thus, it is possible that the paradoxical movement of the septum may partly contribute to the increase of COVV after surgery.

The center of volume movement of the ventricles was measured in Study IV as a measure of differences in pumping between the ventricles. The center of volume movement for the ventricles between end diastole and end systole in the base to apex direction was found to be larger in the right ventricle (13.0±0.7 mm, p<0.001) compared to the left ventricle (7.6±0.4 mm). There was no significant

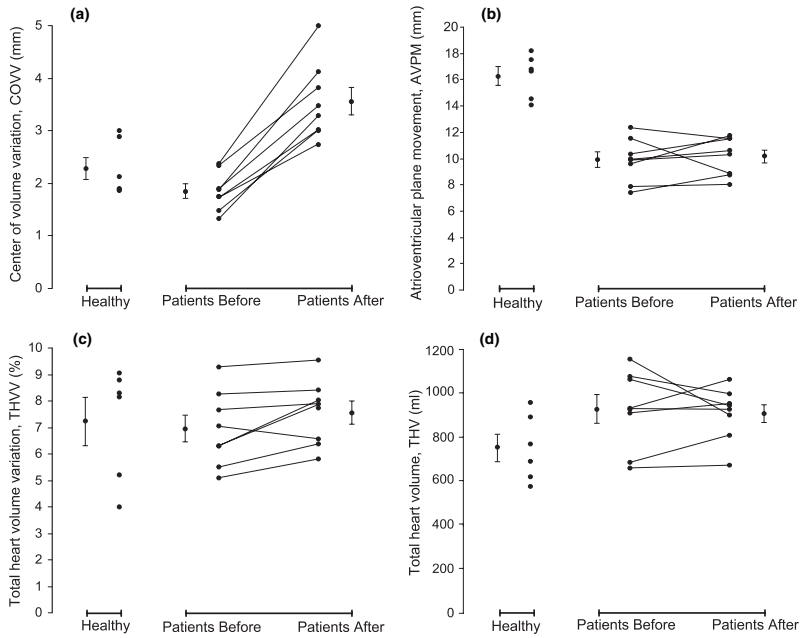

FIGURE 4.4 The COVV, AVPM (synonymous to AVPD) THVV and THV for the healthy subjects and patients before and after cardiac surgery in study II.

difference between the movement in the base-apex direction and the maximum movement in three dimensions for the left or right ventricle (p=0.55 and p=0.39, respectively). The similarity in movement of the ventricular center of volume between the base to apex direction and the maximum movement in three dimensions implies that AVPD explains most of the center of volume movement. The longitudinal shortening of the right ventricle was larger than for the left ventricle, in line with the findings of greater contribution of AVPD to right ventricular pumping compared to the left ventricle (see section 4.4).

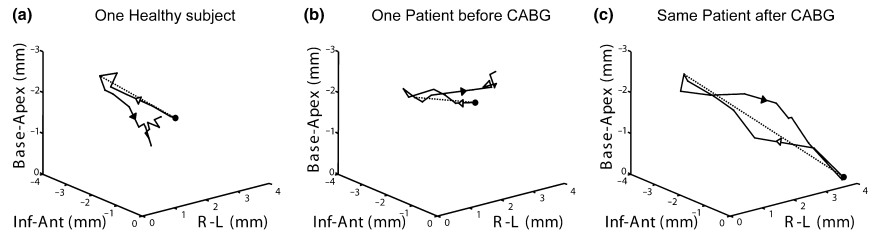

FIGURE 4.5 The COVV throughout the cardiac cycle described a loop in three dimensional space similar in healthy subjects (a) and patients (b). After cardiac surgery the COVV doubled (c). The black dot indicates the COV coordinates at end diastole. The white arrowhead indicate the COVV in systole and the black arrowhead the COVV in diastole. The dotted line indicate the maximum distance between the COV during the cardiac cycle. Note that the COVV loop begins and ends nearly at the same coordinates.

4.3 Atrioventricular plane displacement and apical motion

Studies I, II, III and IV

The longitudinal component of ventricular pumping involves shortening of the ventricle. This can be accomplished by shortening of the base, atrioventricular plane displacement (AVPD) or apical motion. AVPD and apical motion for the left ventricle was investigated in study III. AVPD was compared between athletes, patients and healthy controls in study III. The AVPD of the left ventricle for controls was 16±0 mm. AVPD of the left ventricle was similar in athletes (17±1 mm, p=0.45) and lower in patients (7±1 mm, p<0.001), Figure 4.6. AVPD was greater in the present study (16 mm) compared with a three dimensional transesophageal echocardiographic study by Carlhäll and coworkers (10 mm),[146] and this can be explained by several factors. First, the subjects in that study were older (56±11 years vs. 24±1 years in our study) and AVPD is known to decrease with age.[147] Second, six of the subjects of that study were imaged during general anaesthesia and this could affect AVPD. Last, the AVPD was measured at the mitral annulus in that study and at the tip of the muscular wall in our study which is known to differ.[148] Noteably, the AVPD of the study III is in accordance with recently published normal values of AVPD by MRI.[30] AVPD is known to decrease

with age,[147] and in study III patients were older and had higher heart rates than controls. Thus, part of the difference in AVPD may be related to these disparities. AVPD was studied during breath hold and earlier studies have shown a slight increase in AVPD during inspiration.[149]

Apical motion can contribute to longitudinal shortening but earlier studies have reported the apex to be relatively stationary.[11,41,44,76,150,151] In study I we showed a limited shortening of the entire heart in the apex-base direction during systole (0.9±0.5 %) which also has been reported by others (0.03±1.0 %).[123] Taken together with the limited center of volume movement (2.3±0.2 mm) of the heart during the cardiac cycle (study II), these findings imply that the apical movement can be no more than a few millimetres, and this is confirmed by study III. Study III showed that apical motion between end diastole and end systole was small for controls, athletes and patients (1.9±0.5 mm, 1.8±0.5 mm and 0.1±0.2 mm, respectively). Furthermore, by analysis of the contribution to the SV on an anatomical basis, the apical contribution was found to be negligible. In contrast, a study using epicardially implanted radiopaque markers in sheep reported that apical motion constitutes 22 % of the longitudinal shortening of the ventricle.[152] However, the same study found that isolated AVPD correlated better to ventricular stroke work than AVPD combined with apex movement. This implies that apical epicardial motion is not a large contributor to the SV. Furthermore, it is possible that the increased apical movement found in the mentionend study[152] may be an effect of the surgical preparation with pericardiotomy. Moreover, the epicardial contour of the apex moves very little, although this does not imply that the apical myocardium does not contribute to LV pumping. In conclusion, the AVPD of the LV can be used as an approximation of longitudinal function without taking apical motion in consideration because of the relatively stationary apex.

In study IV a new method for determining the mean AVPD of the right ventricle by MRI was presented. This method takes into account the movement of the septum, the lateral free wall and the right ventricular outflow tract (see Methods 3.5). The AVPD of the right ventricle determined by this method was larger (23.4±0.8 mm, $p<0.001$) compared to the left ventricle (16.4±0.5 mm) which is consistent with earlier studies using echocardiography and MRI.[21,153–155]

4.4 Longitudinal function

Studies III and IV

AVPD has been recognized as an important contributor to LV pumping[8,42,43,45,68]

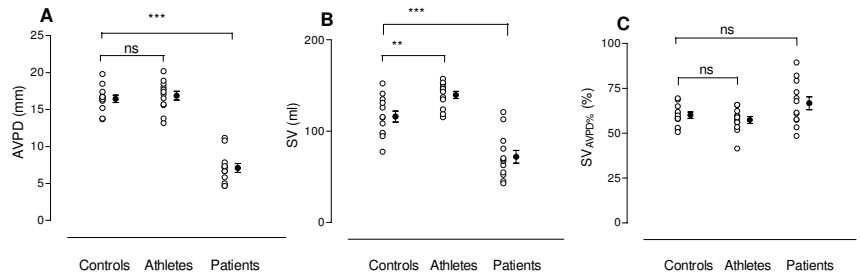

FIGURE 4.6 The atrioventricular plane displacement (AVPD), stroke volume (SV) and percentage contribution to the SV by the AVPD ($SV_{AVPD\%}$) for the left ventricle in controls, athletes and patients. ns $p>0.05$, ** $p<0.01$, *** $p<0.001$

and used as a measure of global LV function,[65–67, 156] but the portion of the LVSV derived by AVPD ($LVSV_{AVPD\%}$) has been unclear.[46, 146, 157, 158] Methodological limitations of echocardiography were discussed by the authors of a study that determined the $LVSV_{AVPD\%}$ to ∼80 %,[46] and in some cases the calculated LVSV derived from the AVPD was larger than the measured total LVSV. Furthermore, the relationship between longitudinal and radial function is affected by heart disease[159] and cardiac function in athletes is different from controls.[34] Therefore, study III was performed to calculate the $LVSV_{AVPD\%}$ in healthy subjects, athletes and patients with dilated cardiomyopathy. The previously proposed derived method[42] was refined and validated against direct measurement of the LVSV generated by AVPD ($LVSV_{AVPD}$) in a subset of the healthy subjects. The $LVSV_{AVPD}$ determined by direct measurement and the derived method did not differ (70±14 ml vs. 68±11 ml, p=0.67). There was a good correlation between the direct measurements and the derived method (r=0.82, p=0.007), and the difference between the direct measurements and the derived method was 2±8 ml. Therefore, the refined derived method was used in all subjects in study III. The $LVSV_{AVPD\%}$ for controls was 60±2 %. $LVSV_{AVPD\%}$ did not differ for athletes (57±2 %, p=0.51) or for patients (67±4 %, p=0.24), Figure 4.6. Interestingly, controls, athletes and patients had similar $LVSV_{AVPD\%}$ although the AVPD was lower in patients compared to controls. This can be explained by a higher SV in athletes, a lower SV in patients compared to controls, the non-significant trend towards larger short-axis areas in athletes, and a significantly larger short-axis areas in patients compared to controls.

Longitudinal function has been proposed to be more important in the right

ventricle compared to the left ventricle,[9, 154, 160] and AVPD has been shown to be larger on the right side compared to the left side.[153] However, no study has quantified the part of the RVSV derived by AVPD ($RVSV_{AVPD}$). Therefore, study IV was designed to determine $RVSV_{AVPD}$ by direct volumetric measurement as well as the derived method used in study III. The $RVSV_{AVPD}$ determined by the volumetric and derived method did not differ (p=0.60) and the difference between the volumetric and derived method was 2.6±7.2 ml (range -11 to 9 ml). There was an excellent correlation between the derived and volumetric method for $RVSV_{AVPD}$ (r=0.92, p<0.001). The amount of right ventricular stroke volume generated by longitudinal AVPD ($RVSV_{AVPD\%}$) was 82±2 % by direct volumetry and 78±2 % by the derived method. The difference between the ventricles is explained by the larger AVPD of the RV compared to the LV, whereas the short-axis areas of the left and right ventricle did not differ. Figure 4.7 shows the proportion of the stroke volume generated by radial function and longitudinal function for each ventricle and the total heart.

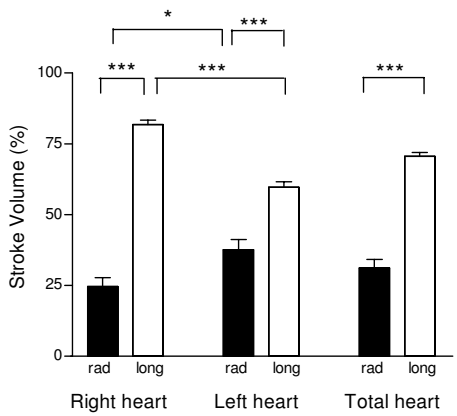

FIGURE 4.7 Percentage contribution to stroke volume by radial (rad) and longitudinal (long) function for the right and left side of the heart as well as the total heart. * p<0.05, *** p<0.001

Radial function in Figure 4.7 is calculated from flow imaging (see section 4.5 below) and thus is independently calculated and also serves as validation. The longitudinal contribution to RVSV, LVSV and TSV was larger than the radial contribution (p<0.001 for all groups). The longitudinal contribution to RVSV

was larger than the longitudinal contribution to LVSV ($p<0.001$), and the radial contribution to LVSV was consequently larger than the radial contribution to RVSV ($p<0.05$). The difference in pumping between the ventricles can be appreciated in Figure 4.8. In conclusion, longitudinal function explains ∼60 % of the left ventricular stroke volume and ∼80 % of the right ventricular stroke volume.

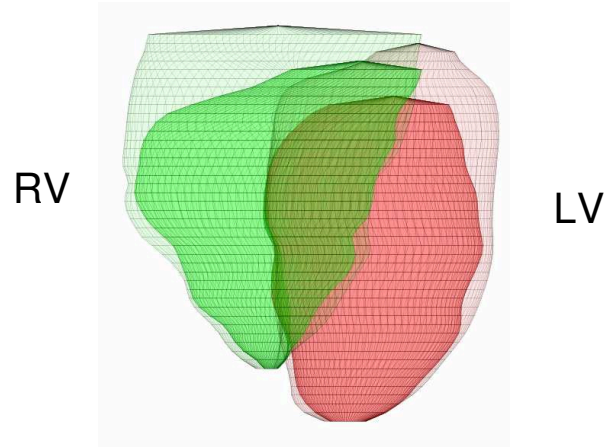

FIGURE 4.8 Three dimensional reconstruction of the epicardial borders of the left ventricle (LV) and right ventricle (RV) in end diastole (open net) and end systole (colored surface).

4.5 Integration of outer and inner volume changes of the heart

Studies I-IV

Studies I and II raised questions regarding the cause of the total heart volume variation (THVV) and why THVV did not differ between healthy subjects and patients with decreased AVPD. Atrial filling is coupled to ventricular ejection by AVPD but the stroke volume generated by radial function, however, does not affect atrial filling. Thus, radial function has been proposed to explain the inward motion of the outer borders of the ventricles[42,46] and hence, total heart volume variation.[123] Study IV was performed to test the hypothesis that the SV caused by radial function explains the outer heart volume variation. THVV was calculated

by the flow and volumetric methods described previously (section 3.3). Figure 4.9 shows the relationship between THVV and the stroke volume generated by radial function (r=0.92, R^2=0.84, p<0.001). The difference between THVV and the stroke volume generated by radial function was 3±13 ml (range -10 to 16 ml) and THVV did not differ significantly from the stroke volume generated by radial function (p=0.66). The R^2 of the relation between THVV and radial function was 0.84. This implies that 84 % of the THVV depends on radial function of the ventricles. The remaining part of the THVV might be explained by THVV at the atrial level or be a measurement error. As discussed in the Introduction and illustrated in Figure 1.3, outer volume changes of the atria will also influence the measurement of THVV. Study I showed that the atria contributed to a small part of the THVV and this is in line with the low COVV found in study II. No atrial contribution to THVV would mean a larger COVV (see Figure 1.3). The reduced outer dimensions of the atria at the time point of minimum THV can be appreciated in Figure 6 in study I and Figure 2 in study IV.

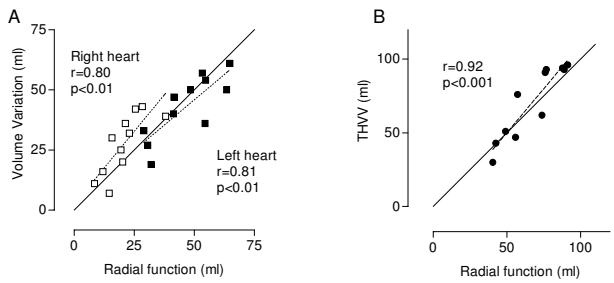

FIGURE 4.9 Relationship between outer volume variations of the heart and radial function of the ventricles. The solid lines indicate the line of identity and the broken lines the regression line. Note that the right heart has lower volume variation and radial function that the left heart.

In studies I and IV the THVV was found to be larger on the left side of the heart (61±2 % and 62±2 % of the THVV, respectively) compared to the right side. This is consistent with the larger longitudinal function, and thus less radial function, found on the right side of the heart compared to the left side. In study III, the longitudinal function of the left ventricle did not differ between healthy subjects and patients with decreased AVPD. Thus, the reason for an unchanged THVV between patients and healthy subjects in study II may be a similar relationship between longitudinal and radial contribution to the SV. Notably, the THVV

differs between subjects and the findings of study IV indicate that this is related to different proportions of radial and longitudinal function between individuals. Furthermore, THVV has been shown to be smaller in smaller species[41, 43, 45] compared to man.[49] Considering the current findings, this implies that radial function is less important in smaller species, and that longitudinal function is the major contributor to SV in these animals.

In conclusion, most of the total heart volume variation from end diastole to minimum THV is explained by the radial component of the ventricular stroke volume although there is a small atrial contribution that lowers COVV. A method for quantifying the radial function of each ventricle by flow imaging of the vessels leading to and from the heart has been presented and validated. In Figure 1.3, five theoretical models of total heart volume variations and cardiac pumping were presented. The results of studies I, II and IV support model E of Figure 1.3 which shows that a combination of radial and longitudinal function contribute to ventricular pumping (Figure 4.7) and that there is a proportional decrease in THV of all parts of the heart during systole (Fig. 6 and 7 of Study I). This is concordant with a minimal COVV (Figure 4.4 and Figure 4.5) and a low THVV (Figure 1.4, Figure 4.4 and Figure 4.10).

4.6 Late ejection filling volume

Study V

The time point of the lowest THV occurs during late systole and close inspection of the flow measurements from study I show that the inflow to the heart begins to exceed the outflow prior to the end of systolic ejection. This results in an increase of THV before the end of systolic ejection, which would mean that the lowest THV does not coincide with end systole. We propose the term late ejection filling volume (LEFV) for this increase in THV which occurs between minimum THV and end systole. Figure 4.10 shows the heart at minimum THV as well as end systole. To our knowledge, the LEFV has not previously been described or quantified and therefore Study V was designed to calculate LEFV. The quantification of the LEFV is illustrated for both sides of the heart and the total heart in Figure 3.2. The LEFV is the difference in inflow and outflow between the time points indicated by the two vertical dotted lines 1 and 2. The LEFV for the total heart was 11.4 ± 1.3 ml which corresponds to 17.8 ± 2.3 % of the THVV or 1.4 ± 0.1 % of the THV. The LEFV of the right and left side of the heart did not differ ($p=0.92$). The LEFV must occur in the atria because of the ongoing ventricular ejection which means that the atrioventricular (AV) valves are closed. Thus, the LEFV may be the result of atrial filling during late systole by blood that

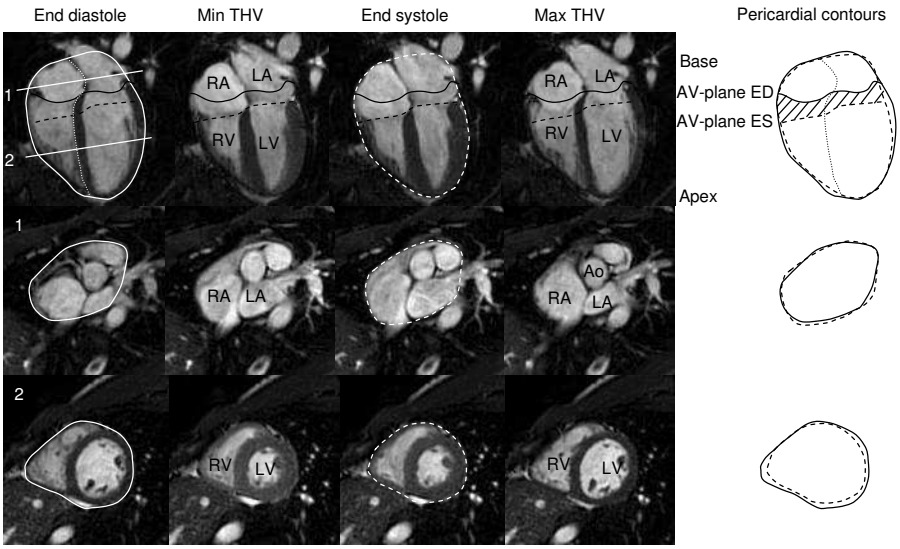

FIGURE 4.10 Cardiac structures and the pericardial contours of the heart throughout the cardiac cycle. The top panels show the heart in a four-chamber view. The two bottom rows show the heart in short-axis views as indicated by the lines 1 and 2 in the top left-hand panel. The pericardial contours and AV-plane is indicated by a solid line at end diastole and by a broken line at end systole. The pericardial contours and the AV-plane in end diastole and end systole are superimposed in the right hand column. The dotted line in the four-chamber view divides the heart into the left and right side. The SV generated by AVPD is indicated by diagonal lines. A heart with a THV of 800 ml and a THVV of 8 % (∼60 ml) generate its TSV of 200 ml (100 ml from each ventricle) by a longitudinal function of 80 % (80 ml) on the right side and 60 % (60 ml) on the left side. This volume is indicated by the diagonal lines in the top right panel. The remaining total stroke volume of 60 ml (200 ml - 80 ml - 60 ml) is generated by radial squeezing that results in a THVV, which can be appreciated as the difference between outer pericardial contours at ventricular level in the right hand column.

was accelerated during earlier systolic AVPD. This could mean that kinetic energy from inflowing venous blood is generated during early systole and the inertia of the blood from the veins causes continued filling in late systole (LEFV) and ultimately early diastole. This may imply that diastolic dysfunction rather may be a diastolic observation of dysfunction during systole which has been under debate.[161,162] A reduction in systolic function would thereby result in a decrease in kinetic energy of the inflowing venous blood which would be observed as a reduced LEFV and a reduced diastolic ventricular filling rate. This hypothesis is supported by previous studies showing a coupling between systolic and early diastolic function[40,163] and decreased longitudinal systolic function in patients with diastolic dysfunction.[164–166] The LEFV may thereby be a novel measure to further understand this connection and may be a new measure of systolic dysfunction. Further studies to elucidate the kinetic energy of blood flow throughout the cardiac cycle in health and disease are therefore merited.

4.7 Atrial wave reversal volume

Study V

The rise in atrial pressure which can be observed by cardiac catheterization during atrial contraction[167] causes reversal of blood out of the heart in late diastole (a-wave reversal) which can be seen using Doppler echocardiography.[20,134,135,168] This reversal results in a late diastolic decrease in the THV and it has been proposed that this results in a neglible change in volume.[23,35] However, the a-wave reversal volume (AWRV) is difficult to measure with Doppler echocardiography[169–171] and therefore has not been quantitatively assessed. The negative flow during late diastole can be seen in the flow data in Figure 3.2 and from these flow measurements the AWRV was calculated in study V. In ten out of eleven subjects, flow out of the heart in the veins was found in late diastole and this coincided with the AVPD caused by atrial contraction (Figure 3.2). The resulting AWRV was greater in the caval veins (4.3±0.6 ml, $p<0.05$) than in the pulmonary veins (2.6±0.7 ml). The resulting volume decrease of the total heart caused by the negative flow in the veins during late diastole was 6.9±1.1 ml. Furthermore, the total AWRV was 11.2±1.9 % of THVV and 0.8±0.1 % of THV. A-wave reversal assessed with Doppler echocardiography has been found to correlate to left ventricular end diastolic filling pressure[172] and right ventricular function,[173] and this implies that the THV decrease during atrial contraction is related to ventricular function.

The presence of an AWRV means that the maximum THV does not occur in end diastole but rather in late diastole before atrial contraction (Figure 4.10). The

THVV reported in this thesis is based on calculations of THV at end diastole and thus the maximum THVV is slightly larger than the reported 5-11 % of study I. However, this does not mean that the findings of previously published studies[23, 35, 123] or study IV must be re-evaluated. The difference between THV in end diastole and minimum THV should still be used when using THVV to calculate systolic radial function. The amount of blood exiting the heart during atrial contraction does not influence the relationship between radial function and THVV during systolic ventricular contraction.

Chapter 5

Conclusions

This thesis has investigated aspects on cardiac pumping that may contribute to the understanding of cardiac pumping efficiency. The thesis has explained the total heart volume variation throughout the cardiac cycle and quantified the contribution of the AV-plane to ventricular pumping. The major conclusions of each paper were:

I. The total heart volume decreases during systole by ∼8 % (range 5-11 %) in humans. The variation in total heart volume change between subjects likely demonstrates a true physiological variation because of the concordant findings from two independent methods.

II. The center of volume during the cardiac cycle describes a well-defined loop in three-dimensional space ∼2 mm between the extreme points. COVV and THVV are similar in patients and healthy individuals. After coronary-bypass surgery, however, COVV approximately doubled while the THVV was nearly unchanged.

III. Longitudinal AVPD is the primary contributor to LV pumping, accounting for ∼60 % of the SV in healthy subjects and this does not differ in athletes or in patients with dilated cardiomyopathy.

IV. Radial function of the ventricles explains over 80 % of the THVV and independent measurements by volumetric and flow methods yielded similar results. The longitudinal component of RV pumping is higher compared to the LV (∼80 % vs. ∼60 %), and is explained by the larger AVPD of the RV.

V. A previously unknown increase in total heart volume before the end of systolic ejection which occurs in the atria has been identified and quantified

to ∼11 ml. This volume might be important for understanding the coupling between systolic and diastolic function. Furthermore, the total heart volume decreases during atrial contraction by ∼7 ml.

Bibliography

[1] Givertz M, Colucci WS, Braunwald E. Clinical Aspects of Heart Failure. In E Braunwald, D Zipes, P Libby, editors, *Heart Disease, A Textbook of Cardiovascular Medicine*, pages 534–561. W.B. Saunders Company, Philadelphia, 6.th edition, 2001.

[2] Swedberg K, Cleland J, Dargie H, Drexler H, Follath F, Komajda M, Tavazzi L, Smiseth OA, Gavazzi A, et al. Guidelines for the diagnosis and treatment of chronic heart failure: executive summary (update 2005): The Task Force for the Diagnosis and Treatment of Chronic Heart Failure of the European Society of Cardiology. *Eur Heart J*, 26(11):1115–40, 2005.

[3] Asplund K, Kärvinge C. *Socialstyrelsens riktlinjer för hjärtsjukvård 2004. Det medicinska faktadokumentet*. 2004.

[4] Cowie MR, Wood DA, Coats AJ, Thompson SG, Poole-Wilson PA, Suresh V, Sutton GC. Incidence and aetiology of heart failure; a population-based study. *Eur Heart J*, 20(6):421–8, 1999.

[5] Hunt SA, Baker DW, Chin MH, Cinquegrani MP, Feldman AM, Francis GS, Ganiats TG, Goldstein S, Gregoratos G, et al. ACC/AHA guidelines for the evaluation and management of chronic heart failure in the adult: executive summary. A report of the American College of Cardiology/American Heart Association Task Force on Practice Guidelines (Committee to revise the 1995 Guidelines for the Evaluation and Management of Heart Failure). *J Am Coll Cardiol*, 38(7):2101–13, 2001.

[6] Buckberg GD, Weisfeldt ML, Ballester M, Beyar R, Burkhoff D, Coghlan HC, Doyle M, Epstein ND, Gharib M, et al. Left ventricular form and function: scientific priorities and strategic planning for development of new views of disease. *Circulation*, 110(14):e333–6, 2004.

[7] Holt JP. The normal pericardium. *Am J Cardiol*, 26(5):455–65, 1970.

[8] Ingels NB. Myocardial fiber architecture and left ventricular function. *Technol Health Care*, 5(1-2):45–52, 1997.

[9] Rushmer RF, Crystal DK, Wagner C. The functional anatomy of ventricular contraction. *Circ Res*, 1(2):162–70, 1953.

[10] Greenbaum RA, Ho SY, Gibson DG, Becker AE, Anderson RH. Left ventricular fibre architecture in man. *Br Heart J*, 45(3):248–63, 1981.

[11] Buckberg GD, Mahajan A, Jung B, Markl M, Hennig J, Ballester-Rodes M. MRI myocardial motion and fiber tracking: a confirmation of knowledge from different imaging modalities. *Eur J Cardiothorac Surg*, 29 Suppl 1:S165–77, 2006.

[12] Torrent-Guasp F, Ballester M, Buckberg GD, Carreras F, Flotats A, Carrio I, Ferreira A, Samuels LE, Narula J. Spatial orientation of the ventricular muscle band: physiologic contribution and surgical implications. *J Thorac Cardiovasc Surg*, 122(2):389–92, 2001.

[13] Coghlan C, Hoffman J. Leonardo da Vinci's flights of the mind must continue: cardiac architecture and the fundamental relation of form and function revisited. *Eur J Cardiothorac Surg*, 29 Suppl 1:S4–17, 2006.

[14] Streeter DD, Spotnitz HM, Patel DP, Ross J, Sonnenblick EH. Fiber orientation in the canine left ventricle during diastole and systole. *Circ Res*, 24(3):339–47, 1969.

[15] Ingels NB, Hansen DE, Daughters GT, Stinson EB, Alderman EL, Miller DC. Relation between longitudinal, circumferential, and oblique shortening and torsional deformation in the left ventricle of the transplanted human heart. *Circ Res*, 64(5):915–27, 1989.

[16] Lunkenheimer PP, Redmann K, Kling N, Jiang X, Rothaus K, Cryer CW, Wubbeling F, Niederer P, Heitz PU, et al. Three-dimensional architecture of the left ventricular myocardium. *Anat Rec A Discov Mol Cell Evol Biol*, 288(6):565–78, 2006.

[17] Widmaier E, Raff H, Strang K. Mechanical events of the cardiac cycle. In *Vander's Human Physiology: The Mechanisms of Body Function, Tenth edition*, pages 404–405. McGraw-Hill Higher Education, New York, 1996.

[18] Guyton A, Hall J. Muscle Blood Flow and Cardiac Output During Exercise; the Coronary Circulation. In *Textbook of Medical Physiology*, pages 223–234. W.B. Saunders Company, Philadelphia, PA19106, 2000.

[19] Opie L. Contractile Performance of the Intact Heart. In E Braunwald, D Zipes, P Libby, editors, *Heart Disease. A Textbook of Cardiovascular Medicine*, page 463. W.B. Saunders Company, Philadelphia, 6:th edition, 2001.

[20] Otto C. Ventricular diastolic filling and function. In *Textbook of Clinical Echocardiography*, pages 166–195. Elsevier Saunders, Philadelphia, 3:rd edition, 2004.

[21] Otto C. Left and right ventricular function. In *Textbook of Clinical Echocardiography*, pages 131–165. Elsevier Saunders, Philadelphia, 3:rd edition, 2004.

[22] Hitch DC, Nolan SP. Descriptive analysis of instantaneous left atrial volume–with special reference to left atrial function. *J Surg Res*, 30(2):110–20, 1981.

[23] Bowman AW, Kovacs SJ. Left atrial conduit volume is generated by deviation from the constant-volume state of the left heart: a combined MRI-echocardiographic study. *Am J Physiol Heart Circ Physiol*, 286(6):H2416–2424, 2004.

[24] Gaynor SL, Maniar HS, Prasad SM, Steendijk P, Moon MR. Reservoir and conduit function of right atrium: impact on right ventricular filling and cardiac output. *Am J Physiol Heart Circ Physiol*, 288(5):H2140–5, 2005.

[25] Nishikawa Y, Roberts JP, Tan P, Klopfenstein CE, Klopfenstein HS. Effect of dynamic exercise on left atrial function in conscious dogs. *J Physiol*, 481 (Pt 2):457–68, 1994.

[26] Prioli A, Marino P, Lanzoni L, Zardini P. Increasing degrees of left ventricular filling impairment modulate left atrial function in humans. *Am J Cardiol*, 82(6):756–61, 1998.

[27] Tseng WY, Liao TY, Wang JL. Normal systolic and diastolic functions of the left ventricle and left atrium by cine magnetic resonance imaging. *J Cardiovasc Magn Reson*, 4(4):443–57, 2002.

[28] Chung CS, Karamanoglu M, Kovacs SJ. Duration of diastole and its phases as a function of heart rate during supine bicycle exercise. *Am J Physiol Heart Circ Physiol*, 287(5):H2003–2008, 2004.

[29] Little W. Assessment of Normal and Abnormal Cardiac Function. In E Braunwald, D Zipes, P Libby, editors, *Heart Disease, A Textbook of Cardiovascular Medicine*, pages 479–502. W.B. Saunders Company, Philadelphia, 6.th edition, 2001.

[30] Maceira A, Prasad SM, Khan M, Pennell DJ. Normalized Left Ventricular Systolic and Diastolic Function by Steady State Free Precession Cardiovascular Magnetic Resonance. *Journal of Cardiovascular Magnetic Resonance*, 8:417–426, 2006.

[31] Bella J, Palmieri V, Kitzman D, Liu J, Oberman A, Hunt S, Hopkins P, Rao D, Arnett D, Devereux R. Gender difference in diastolic function in hypertension (the HyperGEN study). *Am J Cardiol*, 89:1052–1056, 2002.

[32] Kitzman D, Sheikh K, Beere P, Philips J, Higginbotham M. Age-related alterations of Doppler left ventricular filling indexes in normal subjects are independent of left ventricular mass, heart rate, contractility and loading conditions. *J Am Coll Cardiol*, 18:1243–1250, 1991.

[33] Engels G, Muller E, Reynen K, Wilke N, Bachmann K. Evaluation of left ventricular inflow and volume by MR. *Magn Reson Imaging*, 11(7):957–64, 1993.

[34] Jensen-Urstad M, Bouvier F, Nejat M, Saltin B, Brodin LA. Left ventricular function in endurance runners during exercise. *Acta Physiol Scand*, 164(2):167–72, 1998.

[35] Riordan MM, Kovacs SJ. Relationship of pulmonary vein flow to left ventricular short-axis epicardial displacement in diastole: model-based prediction with in vivo validation. *Am J Physiol Heart Circ Physiol*, 291(3):H1210–1215, 2006.

[36] Kilner PJ, Henein MY, Gibson DG. Our tortuous heart in dynamic mode–an echocardiographic study of mitral flow and movement in exercising subjects. *Heart Vessels*, 12(3):103–10, 1997.

[37] Channer KS, Jones JV. The contribution of atrial systole to mitral diastolic blood flow increases during exercise in humans. *J Physiol*, 411:53–61, 1989.

[38] Fyrenius A, Wigstrom L, Ebbers T, Karlsson M, Engvall J, Bolger AF. Three dimensional flow in the human left atrium. *Heart*, 86(4):448–55, 2001.

[39] Wigstrom L, Ebbers T, Fyrenius A, Karlsson M, Engvall J, Wranne B, Bolger AF. Particle trace visualization of intracardiac flow using time-resolved 3D phase contrast MRI. *Magn Reson Med*, 41(4):793–9, 1999.

[40] Kilner PJ, Yang GZ, Wilkes AJ, Mohiaddin RH, Firmin DN, Yacoub MH. Asymmetric redirection of flow through the heart. *Nature*, 404(6779):759–61, 2000.

[41] Hoffman EA, Ritman EL. Invariant total heart volume in the intact thorax. *Am J Physiol*, 249(4 Pt 2):H883–90, 1985.

[42] Lundback S. Cardiac Pumping and Function of the Ventricular Septum. *Acta Physiologica Scandinavica*, 127:8–101, 1986.

[43] Hamilton WF, Rompf JH. Movement of the base of the ventricle and the relative constancy of the cardiac volume. *Am J Physiol*, 102:559–565, 1932.

[44] Hoffman EA, Ritman EL. Heart-lung interaction: effect on regional lung air content and total heart volume. *Ann Biomed Eng*, 15(3-4):241–57, 1987.

[45] Gauer OH. Volume Changes of the Left Ventricle During Blood Pooling and Exercise in the Intact Animal - Their Effects on Left Ventricular Performance. *Physiological Reviews*, 35(1):143–155, 1955.

[46] Emilsson K, Brudin L, Wandt B. The mode of left ventricular pumping: is there an outer contour change in addition to the atrioventricular plane displacement? *Clinical Physiology*, 21(4):437–446, 2001.

[47] Hoffman EA, Rumberger J, Dougherty L, Reichek N, Axel L. A geometric view of cardiac "efficiency". *J Am Coll Cardiol*, 13:86A, 1989.

[48] Leithner C, Podolsky A, Globits S, Frank H, Neuhold A, Pidlich J, Schuster E, Staudinger T, Rintelen C, et al. Magnetic-Resonance-Imaging of the Heart During Positive End- Expiratory Pressure Ventilation in Normal Subjects. *Critical Care Medicine*, 22(3):426–432, 1994.

[49] Bowman AW, Kovacs SJ. Assessment and consequences of the constant-volume attribute of the four-chambered heart. *Am J Physiol Heart Circ Physiol*, 285(5):H2027–33, 2003.

[50] Janicki JS, Weber KT. The pericardium and ventricular interaction, distensibility, and function. *Am J Physiol*, 238(4):H494–503, 1980.

[51] Smiseth OA, Frais MA, Kingma I, Smith ER, Tyberg JV. Assessment of pericardial constraint in dogs. *Circulation*, 71(1):158–64, 1985.

[52] Shirato K, Shabetai R, Bhargava V, Franklin D, Ross J. Alteration of the left ventricular diastolic pressure-segment length relation produced by the pericardium. Effects of cardiac distension and afterload reduction in conscious dogs. *Circulation*, 57(6):1191–8, 1978.

[53] Maughan WL, Kallman CH, Shoukas A. The effect of right ventricular filling on the pressure-volume relationship of ejecting canine left ventricle. *Circ Res*, 49(2):382–8, 1981.

[54] Glantz SA, Misbach GA, Moores WY, Mathey DG, Lekven J, Stowe DF, Parmley WW, Tyberg JV. The pericardium substantially affects the left ventricular diastolic pressure-volume relationship in the dog. *Circ Res*, 42(3):433–41, 1978.

[55] Berglund E, Sarnoff SJ, Isaacs JP. Ventricular function: role of the pericardium in regulation of cardiovascular hemodynamics. *Circ Res*, 3(2):133–9, 1955.

[56] Fellows KE, Fogel MA. Mr-Imaging and Heart Function in Patients Pre-Fontan and Post- Fontan Surgery. *Acta Paediatrica*, 84:57–59, 1995.

[57] Fogel MA, Weinberg PM, Fellows KE, Hoffman EA. Magnetic-Resonance-Imaging of Constant Total Heart-Volume and Center-of-Mass in Patients with Functional Single Ventricle before and after Staged Fontan Procedure. *American Journal of Cardiology*, 72(18):1435–1443, 1993.

[58] McDonald IG. The shape and movements of the human left ventricle during systole. A study by cineangiography and by cineradiography of epicardial markers. *Am J Cardiol*, 26(3):221–30, 1970.

[59] Henein MY, Gibson DG. Normal long axis function. *Heart*, 81(2):111–3, 1999.

[60] Wandt B. Long-axis contraction of the ventricles: A modern approach, but described already by Leonardo da Vinci. *Journal of the American Society of Echocardiography*, 13(7):699–706, 2000.

[61] Lind B, Eriksson M, Roumina S, Nowak J, Brodin LA. Longitudinal isovolumic displacement of the left ventricular myocardium assessed by tissue velocity echocardiography in healthy individuals. *J Am Soc Echocardiogr*, 19(3):255–65, 2006.

[62] Holmgren B. The movement of the mitro-aortic ring recorded simultaneosly by cineroentgenography and electrocardiography. *Acta Radiologica*, 27:171–176, 1946.

[63] Odqvist H. A roentgen cinematographic study of the movements of the mitral ring during heart action. *Acta Radiologica*, 26:392–396, 1945.

[64] Zaky A, Grabhorn L, Feigenbaum H. Movement of the mitral ring: a study in ultrasoundcardiography. *Cardiovasc Res*, 1(2):121–31, 1967.

[65] Alam M, Hoglund C, Thorstrand C, Philip A. Atrioventricular plane displacement in severe congestive heart failure following dilated cardiomyopathy or myocardial infarction. *J Intern Med*, 228(6):569–75, 1990.

[66] Alam M, Rosenhamer G. Atrioventricular plane displacement and left ventricular function. *J Am Soc Echocardiogr*, 5(4):427–33, 1992.

[67] Simonson JS, Schiller NB. Descent of the base of the left ventricle: an echocardiographic index of left ventricular function. *J Am Soc Echocardiogr*, 2(1):25–35, 1989.

[68] Henein MY, Gibson DG. Long axis function in disease. *Heart*, 81(3):229–31, 1999.

[69] Sabbah HN, Marzilli M, Stein PD. The relative role of subendocardium and subepicardium in left ventricular mechanics. *Am J Physiol*, 240(6):H920–6, 1981.

[70] Hartley CJ, Latson LA, Michael LH, Seidel CL, Lewis RM, Entman ML. Doppler measurement of myocardial thickening with a single epicardial transducer. *Am J Physiol*, 245(6):H1066–72, 1983.

[71] Sundblad P, Wranne B. Influence of posture on left ventricular long- and short-axis shortening. *Am J Physiol Heart Circ Physiol*, 283(4):H1302–6, 2002.

[72] Popovic ZB, Sun JP, Yamada H, Drinko J, Mauer K, Greenberg NL, Cheng Y, Moravec CS, Penn MS, et al. Differences in left ventricular long-axis function from mice to humans follow allometric scaling to ventricular size. *J Physiol*, 568(Pt 1):255–65, 2005.

[73] Gallagher KP, Osakada G, Matsuzaki M, Miller M, Kemper WS, Ross J J. Nonuniformity of inner and outer systolic wall thickening in conscious dogs. *Am J Physiol*, 249(2 Pt 2):H241–8, 1985.

[74] Myers JH, Stirling MC, Choy M, Buda AJ, Gallagher KP. Direct measurement of inner and outer wall thickening dynamics with epicardial echocardiography. *Circulation*, 74(1):164–72, 1986.

[75] Dumesnil JG, Shoucri RM, Laurenceau JL, Turcot J. A mathematical model of the dynamic geometry of the intact left ventricle and its application to clinical data. *Circulation*, 59(5):1024–34, 1979.

[76] Gorman JH, Gupta KB, Streicher JT, Gorman RC, Jackson BM, Ratcliffe MB, Bogen DK, Edmunds LH. Dynamic three-dimensional imaging of the mitral valve and left ventricle by rapid sonomicrometry array localization. *J Thorac Cardiovasc Surg*, 112(3):712–26, 1996.

[77] Ingels NB, Daughters GT, Stinson EB, Alderman EL. Measurement of midwall myocardial dynamics in intact man by radiography of surgically implanted markers. *Circulation*, 52(5):859–67, 1975.

[78] Lorenz CH, Pastorek JS, Bundy JM. Delineation of normal human left ventricular twist throughout systole by tagged cine magnetic resonance imaging. *J Cardiovasc Magn Reson*, 2(2):97–108, 2000.

[79] Hansen DE, Daughters GT, Alderman EL, Ingels NB, Stinson EB, Miller DC. Effect of volume loading, pressure loading, and inotropic stimulation on left ventricular torsion in humans. *Circulation*, 83(4):1315–26, 1991.

[80] Gilman G, Khandheria BK, Hagen ME, Abraham TP, Seward JB, Belohlavek M. Strain rate and strain: a step-by-step approach to image and data acquisition. *J Am Soc Echocardiogr*, 17(9):1011–20, 2004.

[81] Sutherland GR, Di Salvo G, Claus P, D'Hooge J, Bijnens B. Strain and strain rate imaging: a new clinical approach to quantifying regional myocardial function. *J Am Soc Echocardiogr*, 17(7):788–802, 2004.

[82] Brodin LA. Tissue Doppler, a fundamental tool for parametric imaging. *Clin Physiol Funct Imaging*, 24(3):147–55, 2004.

[83] Selskog P, Heiberg E, Ebbers T, Wigstrom L, Karlsson M. Kinematics of the heart: strain-rate imaging from time-resolved three-dimensional phase contrast MRI. *IEEE Trans Med Imaging*, 21(9):1105–9, 2002.

[84] Bergvall E, Cain P, Arheden H, Sparr G. A fast and highly automated approach to myocardial motion analysis using phase contrast magnetic resonance imaging. *J Magn Reson Imaging*, 23(5):652–61, 2006.

[85] Carlsson M, Ugander M, Mosen H, Buhre T, Arheden H. Atrioventricular Plane Displacement is the Major Contributor to Left Ventricular Pumping in Healthy Adults, Athletes and Patients with Dilated Cardiomyopathy. *Am J Physiol Heart Circ Physiol*, page 01148.2006, 2006.

[86] Forbat SM, Sakrana MA, Darasz KH, El-Demerdash F, Underwood SR. Rapid assessment of left ventricular volume by short axis cine MRI. *Br J Radiol*, 69(819):221–5, 1996.

[87] Lawson MA, Blackwell GG, Davis ND, Roney M, Dell'Italia LJ, Pohost GM. Accuracy of biplane long-axis left ventricular volume determined by cine magnetic resonance imaging in patients with regional and global dysfunction. *Am J Cardiol*, 77(12):1098–104, 1996.

[88] Sievers B, Brandts B, Franken U, Trappe HJ. Single and biplane TrueFISP cardiovascular magnetic resonance for rapid evaluation of left ventricular volumes and ejection fraction. *J Cardiovasc Magn Reson*, 6(3):593–600, 2004.

[89] Chuang ML, Hibberd MG, Salton CJ, Beaudin RA, Riley MF, Parker RA, Douglas PS, Manning WJ. Importance of imaging method over imaging modality in noninvasive determination of left ventricular volumes and ejection fraction: assessment by two- and three-dimensional echocardiography and magnetic resonance imaging. *J Am Coll Cardiol*, 35(2):477–84, 2000.

[90] Semelka RC, Tomei E, Wagner S, Mayo J, Kondo C, Suzuki J, Caputo GR, Higgins CB. Normal left ventricular dimensions and function: interstudy reproducibility of measurements with cine MR imaging. *Radiology*, 174(3 Pt 1):763–8, 1990.

[91] Longmore DB, Klipstein RH, Underwood SR, Firmin DN, Hounsfield GN, Watanabe M, Bland C, Fox K, Poole-Wilson PA, et al. Dimensional accuracy of magnetic resonance in studies of the heart. *Lancet*, 1(8442):1360–2, 1985.

[92] Rehr RB, Malloy CR, Filipchuk NG, Peshock RM. Left ventricular volumes measured by MR imaging. *Radiology*, 156(3):717–9, 1985.

[93] Katz J, Milliken MC, Stray-Gundersen J, Buja LM, Parkey RW, Mitchell JH, Peshock RM. Estimation of human myocardial mass with MR imaging. *Radiology*, 169(2):495–8, 1988.

[94] Milliken MC, Stray-Gundersen J, Peshock RM, Katz J, Mitchell JH. Left ventricular mass as determined by magnetic resonance imaging in male endurance athletes. *Am J Cardiol*, 62(4):301–5, 1988.

[95] Katz J, Whang J, Boxt LM, Barst RJ. Estimation of right ventricular mass in normal subjects and in patients with primary pulmonary hypertension by nuclear magnetic resonance imaging. *J Am Coll Cardiol*, 21(6):1475–81, 1993.

[96] Bottini PB, Carr AA, Prisant LM, Flickinger FW, Allison JD, Gottdiener JS. Magnetic resonance imaging compared to echocardiography to assess left ventricular mass in the hypertensive patient. *Am J Hypertens*, 8(3):221–8, 1995.

[97] Bellenger NG, Davies LC, Francis JM, Coats AJ, Pennell DJ. Reduction in sample size for studies of remodeling in heart failure by the use of cardiovascular magnetic resonance. *J Cardiovasc Magn Reson*, 2(4):271–8, 2000.

[98] Bogaert JG, Bosmans HT, Rademakers FE, Bellon EP, Herregods MC, Verschakelen JA, Van de Werf F, Marchal GJ. Left ventricular quantification with breath-hold MR imaging: comparison with echocardiography. *Magma*, 3(1):5–12, 1995.

[99] Bowman AW, Kovacs SJ. Prediction and assessment of the time-varying effective pulmonary vein area via cardiac MRI and Doppler echocardiography. *Am J Physiol Heart Circ Physiol*, 288(1):H280–286, 2005.

[100] Lorenz CH, Walker ES, Morgan VL, Klein SS, Graham TP. Normal human right and left ventricular mass, systolic function, and gender differences by cine magnetic resonance imaging. *J Cardiovasc Magn Reson*, 1(1):7–21, 1999.

[101] Cain PA, Ahl R, Hedstrom E, Ugander M, Allansdotter-Johnsson A, Friberg P, Marild S, Arheden H. Physiological determinants of the variation in left ventricular mass from early adolescence to late adulthood in healthy subjects. *Clin Physiol Funct Imaging*, 25(6):332–9, 2005.

[102] Hundley WG, Li HF, Hillis LD, Meshack BM, Lange RA, Willard JE, Landau C, Peshock RM. Quantitation of cardiac output with velocity-encoded, phase-difference magnetic resonance imaging. *Am J Cardiol*, 75(17):1250–5, 1995.

[103] Arheden H, Holmqvist C, Thilen U, Hanseus K, Bjorkhem G, Pahlm O, Laurin S, Stahlberg F. Left-to-right cardiac shunts: comparison of measurements obtained with MR velocity mapping and with radionuclide angiography. *Radiology*, 211(2):453–8, 1999.

[104] Sondergaard L, Hildebrandt P, Lindvig K, Thomsen C, Stahlberg F, Kassis E, Henriksen O. Valve area and cardiac output in aortic stenosis: quantification by magnetic resonance velocity mapping. *Am Heart J*, 126(5):1156–64, 1993.

[105] Rebergen SA, van der Wall EE, Helbing WA, de Roos A, van Voorthuisen AE. Quantification of pulmonary and systemic blood flow by magnetic resonance velocity mapping in the assessment of atrial-level shunts. *Int J Card Imaging*, 12(3):143–52, 1996.

[106] Van Rossum AC, Sprenger M, Visser FC, Peels KH, Valk J, Roos JP. An in vivo validation of quantitative blood flow imaging in arteries and veins using magnetic resonance phase-shift techniques. *Eur Heart J*, 12(2):117–26, 1991.

[107] Evans AJ, Iwai F, Grist TA, Sostman HD, Hedlund LW, Spritzer CE, Negro-Vilar R, Beam CA, Pelc NJ. Magnetic resonance imaging of blood flow with a phase subtraction technique. In vitro and in vivo validation. *Invest Radiol*, 28(2):109–15, 1993.

[108] Kondo C, Caputo GR, Semelka R, Foster E, Shimakawa A, Higgins CB. Right and left ventricular stroke volume measurements with velocity-encoded cine MR imaging: in vitro and in vivo validation. *AJR Am J Roentgenol*, 157(1):9–16, 1991.

[109] Firmin DN, Nayler GL, Klipstein RH, Underwood SR, Rees RS, Longmore DB. In vivo validation of MR velocity imaging. *J Comput Assist Tomogr*, 11(5):751–6, 1987.

[110] Bogren HG, Klipstein RH, Firmin DN, Mohiaddin RH, Underwood SR, Rees RS, Longmore DB. Quantitation of antegrade and retrograde blood flow in the human aorta by magnetic resonance velocity mapping. *Am Heart J*, 117(6):1214–22, 1989.

[111] Brenner LD, Caputo GR, Mostbeck G, Steiman D, Dulce M, Cheitlin MD, O'Sullivan M, Higgins CB. Quantification of left to right atrial shunts with velocity-encoded cine nuclear magnetic resonance imaging. *J Am Coll Cardiol*, 20(5):1246–50, 1992.

[112] Lund GK, Wendland MF, Shimakawa A, Arheden H, Stahlberg F, Higgins CB, Saeed M. Coronary sinus flow measurement by means of velocity-encoded cine MR imaging: validation by using flow probes in dogs. *Radiology*, 217(2):487–93, 2000.

[113] Schwitter J, DeMarco T, Kneifel S, von Schulthess GK, Jorg MC, Arheden H, Ruhm S, Stumpe K, Buck A, et al. Magnetic resonance-based assessment of global coronary flow and flow reserve and its relation to left ventricular functional parameters: a comparison with positron emission tomography. *Circulation*, 101(23):2696–702, 2000.

[114] Arheden H, Saeed M, Tornqvist E, Lund G, Wendland MF, Higgins CB, Stahlberg F. Accuracy of segmented MR velocity mapping to measure small vessel pulsatile flow in a phantom simulating cardiac motion. *J Magn Reson Imaging*, 13(5):722–8, 2001.

[115] Razavi R, Hill DL, Keevil SF, Miquel ME, Muthurangu V, Hegde S, Rhode K, Barnett M, van Vaals J, et al. Cardiac catheterisation guided by MRI in children and adults with congenital heart disease. *Lancet*, 362(9399):1877–82, 2003.

[116] Kuehne T, Yilmaz S, Schulze-Neick I, Wellnhofer E, Ewert P, Nagel E, Lange P. Magnetic resonance imaging guided catheterisation for assessment of pulmonary vascular resistance: in vivo validation and clinical application in patients with pulmonary hypertension. *Heart*, 91(8):1064–9, 2005.

[117] Nayler GL, Firmin DN, Longmore DB. Blood flow imaging by cine magnetic resonance. *J Comput Assist Tomogr*, 10(5):715–22, 1986.

[118] Ugander M, Cain PA, Perron A, Hedstrom E, Arheden H. Infarct transmurality and adjacent segmental function as determinants of wall thickening in revascularized chronic ischemic heart disease. *Clin Physiol Funct Imaging*, 25(4):209–14, 2005.

[119] Bloomgarden DC, Fayad ZA, Ferrari VA, Chin B, Sutton MG, Axel L. Global cardiac function using fast breath-hold MRI: validation of new acquisition and analysis techniques. *Magn Reson Med*, 37(5):683–92, 1997.

[120] Clay S, Alfakih K, Radjenovic A, Jones T, Ridgway JP, Sinvananthan MU. Normal range of human left ventricular volumes and mass using steady state free precession MRI in the radial long axis orientation. *Magma*, 19(1):41–5, 2006.

[121] Pennell DJ. Ventricular volume and mass by CMR. *J Cardiovasc Magn Reson*, 4(4):507–13, 2002.

[122] Shors S, Fung C, Francois C, Finn J, Fieno D. Accurate Quantification of Right Ventricular Mass at MR Imaging by Using Cine True Fast Imaging with Steady-State Precession: Study in Dogs. *Radiology*, 230:383–388, 2004.

[123] Waters EA, Bowman AW, Kovacs SJ. MRI-determined left ventricular "crescent effect": a consequence of the slight deviation of contents of the pericardial sack from the constant-volume state. *Am J Physiol Heart Circ Physiol*, 288(2):H848–853, 2005.

[124] Heiberg E, Wigström L, Carlsson M, Bolger AF, Karlsson M. Time Resolved Three-dimensional Automated Segmentation of the Left Ventricle. *In Proceedings of IEEE Computers in Cardiology*, 32:599–602, 2005.

[125] Shrout P, Fleiss J. Intraclass correlations - uses in assessing rater reliability. *Psychological Bulletin*, 86(2):420–428, 1979.

[126] Bland JM, Altman DG. Statistical methods for assessing agreement between two methods of clinical measurement. *Lancet*, 1(8476):307–10, 1986.

[127] Beloucif S, Takata M, Shimada M, Robotham JL. Influence of Pericardial Constraint on Atrioventricular Interactions. *American Journal of Physiology*, 263(1):H125–H134, 1992.

[128] Beyar R, Hausknecht MJ, Halperin HR, Yin FCP, Weisfeldt ML. Interaction between Cardiac Chambers and Thoracic Pressure in Intact Circulation. *American Journal of Physiology*, 253(5):H1240–H1252, 1987.

[129] Baker AE, Dani R, Smith ER, Tyberg JV, Belenkie I. Quantitative assessment of independent contributions of pericardium and septum to direct ventricular interaction. *Am J Physiol*, 275(2 Pt 2):H476–83, 1998.

[130] Belenkie I, Kieser TM, Sas R, Smith ER, Tyberg JV. Evidence for left ventricular constraint during open heart surgery. *Can J Cardiol*, 18(9):951–9, 2002.

[131] Kroeker CA, Shrive NG, Belenkie I, Tyberg JV. Pericardium modulates left and right ventricular stroke volumes to compensate for sudden changes in atrial volume. *Am J Physiol Heart Circ Physiol*, 284(6):H2247–54, 2003.

[132] Sivaciyan V, Ranganathan N. Transcutaneous doppler jugular venous flow velocity recording. *Circulation*, 57(5):930–9, 1978.

[133] Jarvinen V, Kupari M, Hekali P, Poutanen VP. Assessment of left atrial volumes and phasic function using cine magnetic resonance imaging in normal subjects. *Am J Cardiol*, 73(15):1135–8, 1994.

[134] Bartzokis T, Lee R, Yeoh TK, Grogin H, Schnittger I. Transesophageal echo-Doppler echocardiographic assessment of pulmonary venous flow patterns. *J Am Soc Echocardiogr*, 4(5):457–64, 1991.

[135] Appleton CP. Hemodynamic determinants of Doppler pulmonary venous flow velocity components: new insights from studies in lightly sedated normal dogs. *J Am Coll Cardiol*, 30(6):1562–74, 1997.

[136] Brecher GA. Cardiac Variations in Venous Return Studied with a New Bristle Flowmeter. *American Journal of Physiology*, 176(3):423–430, 1954.

[137] Nilsson NJ, Kurt K. Stromvolumpulse der herznahen Venen bei verschiedenen Kreislaufzuständen. *Zeitschrift Biologie*, 106:386–394, 1954.

[138] Quintana M, Gustafsson T, Sundblad P, Langanger J. The effects of heart rate on myocardial velocity and atrio-ventricular displacement during exercise with and without beta-blockade: a tissue Doppler echocardiographic study. *Eur J Echocardiogr*, 6(2):127–33, 2005.

[139] Slordahl SA, Madslien VO, Stoylen A, Kjos A, Helgerud J, Wisloff U. Atrioventricular plane displacement in untrained and trained females. *Med Sci Sports Exerc*, 36(11):1871–5, 2004.

[140] Waggoner AD, Shah AA, Schuessler JS, Crawford ES, Nelson JG, Miller RR, Quinones MA. Effect of cardiac surgery on ventricular septal motion: assessment by intraoperative echocardiography and cross-sectional two-dimensional echocardiography. *Am Heart J*, 104(6):1271–8, 1982.

[141] Feneley M, Kearney L, Farnsworth A, Shanahan M, Chang V. Mechanisms of the development and resolution of paradoxical interventricular septal motion after uncomplicated cardiac surgery. *Am Heart J*, 114(1 Pt 1):106–14, 1987.

[142] Lehmann KG, Lee FA, McKenzie WB, Barash PG, Prokop EK, Durkin MA, Ezekowitz MD. Onset of altered interventricular septal motion during cardiac surgery. Assessment by continuous intraoperative transesophageal echocardiography. *Circulation*, 82(4):1325–34, 1990.

[143] Force T, Bloomfield P, O'Boyle JE, Pietro DA, Dunlap RW, Khuri SF, Parisi AF. Quantitative two-dimensional echocardiographic analysis of motion and thickening of the interventricular septum after cardiac surgery. *Circulation*, 68(5):1013–20, 1983.

[144] Wranne B, Pinto FJ, Siegel LC, Miller DC, Schnittger I. Abnormal postoperative interventricular motion: new intraoperative transesophageal echocardiographic evidence supports a novel hypothesis. *Am Heart J*, 126(1):161–7, 1993.

[145] Kingma I, Tyberg JV, Smith ER. Effects of diastolic transseptal pressure gradient on ventricular septal position and motion. *Circulation*, 68(6):1304–14, 1983.

[146] Carlhall C, Wigstrom L, Heiberg E, Karlsson M, Bolger AF, Nylander E. Contribution of mitral annular excursion and shape dynamics to total left ventricular volume change. *Am J Physiol Heart Circ Physiol*, 287(4):H1836–41, 2004.

[147] Wandt B, Bojo L, Wranne B. Influence of body size and age on mitral ring motion. *Clin Physiol*, 17(6):635–46, 1997.

[148] Emilsson K, Kahari A, Wandt B. Comparison between circumflex artery motion and mitral annulus motion. *Scand Cardiovasc J*, 35(5):318–25, 2001.

[149] Wandt B, Bojo L, Wranne B. Long and short axis dimensions of the left ventricle change in opposite ways during respiration. *Acta Physiologica Scandinavica*, 162(1):9–12, 1998.

[150] Rogers WJ, Shapiro EP, Weiss JL, Buchalter MB, Rademakers FE, Weisfeldt ML, Zerhouni EA. Quantification of and correction for left ventricular systolic long-axis shortening by magnetic resonance tissue tagging and slice isolation. *Circulation*, 84(2):721–31, 1991.

[151] Slager CJ, Hooghoudt TE, Serruys PW, Schuurbiers JC, Reiber JH, Meester GT, Verdouw PD, Hugenholtz PG. Quantitative assessment of regional left ventricular motion using endocardial landmarks. *J Am Coll Cardiol*, 7(2):317–26, 1986.

[152] Rodriguez F, Tibayan FA, Glasson JR, Liang D, Daughters GT, Ingels NB, Miller DC. Fixed-apex mitral annular descent correlates better with left ventricular systolic function than does free-apex left ventricular long-axis shortening. *J Am Soc Echocardiogr*, 17(2):101–7, 2004.

[153] Hammarstrom E, Wranne B, Pinto FJ, Puryear J, Popp RL. Tricuspid annular motion. *J Am Soc Echocardiogr*, 4(2):131–9, 1991.

[154] Kukulski T, Hubbert L, Arnold M, Wranne B, Hatle L, Sutherland GR. Normal regional right ventricular function and its change with age: a Doppler myocardial imaging study. *J Am Soc Echocardiogr*, 13(3):194–204, 2000.

[155] Voelkel NF, Quaife RA, Leinwand LA, Barst RJ, McGoon MD, Meldrum DR, Dupuis J, Long CS, Rubin LJ, et al. Right ventricular function and failure: report of a National Heart, Lung, and Blood Institute working group on cellular and molecular mechanisms of right heart failure. *Circulation*, 114(17):1883–91, 2006.

[156] Emilsson K, Alam M, Wandt B. The relation between mitral annulus motion and ejection fraction: a nonlinear function. *J Am Soc Echocardiogr*, 13(10):896–901, 2000.

[157] Carlhall C, Wigstrom L, Heiberg E, Karlsson M, Bolger AF, Nylander E. REPLY. *Am J Physiol Heart Circ Physiol*, 291(5):H2551–2552, 2006.

[158] Wandt B, Brodin LA, Lundback S. Misinterpretation About the Contribution of the Left Ventricular Long-Axis Shortening to the Stroke Volume. *Am J Physiol Heart Circ Physiol*, 291(5):H2550–, 2006.

[159] Jones CJ, Raposo L, Gibson DG. Functional importance of the long axis dynamics of the human left ventricle. *Br Heart J*, 63(4):215–20, 1990.

[160] Lindqvist P, Morner S, Karp K, Waldenstrom A. New aspects of septal function by using 1-dimensional strain and strain rate imaging. *J Am Soc Echocardiogr*, 19(11):1345–9, 2006.

[161] Aurigemma GP, Zile MR, Gaasch WH. Contractile Behavior of the Left Ventricle in Diastolic Heart Failure: With Emphasis on Regional Systolic Function. *Circulation*, 113(2):296–304, 2006.

[162] Vinereanu D, Nicolaides E, Tweddel AC, Fraser AG. "Pure" diastolic dysfunction is associated with long-axis systolic dysfunction. Implications for the diagnosis and classification of heart failure. *Eur J Heart Fail*, 7(5):820–8, 2005.

[163] Winter R, Gudmundsson P, Ericsson G, Willenheimer R. Correlation of the M-mode atrioventricular plane early diastolic downward slope and systolic parameters. Coupling of LV systolic and early diastolic function. *Int J Cardiovasc Imaging*, 20(2):101–6, 2004.

[164] Yip G, Wang M, Zhang Y, Fung JWH, Ho PY, Sanderson JE. Left ventricular long axis function in diastolic heart failure is reduced in both diastole and systole: time for a redefinition? *Heart*, 87(2):121–125, 2002.

[165] Nikitin NP, Witte KK, Clark AL, Cleland JG. Color tissue Doppler-derived long-axis left ventricular function in heart failure with preserved global systolic function. *Am J Cardiol*, 90(10):1174–7, 2002.

[166] Yip GW, Zhang Y, Tan PY, Wang M, Ho PY, Brodin LA, Sanderson JE. Left ventricular long-axis changes in early diastole and systole: impact of systolic function on diastole. *Clin Sci (Lond)*, 102(5):515–22, 2002.

[167] Davidson J, Bonow RO. Cardiac Catheterization. In E Braunwald, D Zipes, P Libby, editors, *Heart Disease, A Textbook of Cardiovascular Medicine*, pages 359–386. W.B. Saunders Company, Philadelphia, 6.th edition, 2001.

[168] Sohn DW, Choi RK, Kim YJ. Mechanism and incidence of notched pulmonary venous atrial reversal wave. *J Am Soc Echocardiogr*, 16(1):77–9, 2003.

[169] Gentile F, Mantero A, Lippolis A, Ornaghi M, Azzollini M, Barbier P, Beretta L, Casazza F, Corno R, et al. Pulmonary venous flow velocity patterns in 143 normal subjects aged 20 to 80 years old. An echo 2D colour Doppler cooperative study. *Eur Heart J*, 18(1):148–64, 1997.

[170] Bukachi F, Waldenstrom A, Morner S, Lindqvist P, Henein MY, Kazzam E. Pulmonary venous flow reversal and its relationship to atrial mechanical function in normal subjects–Umea General Population Heart Study. *Eur J Echocardiogr*, 6(2):107–16, 2005.

[171] Appleton CP, Hatle LK, Popp RL. Superior vena cava and hepatic vein Doppler echocardiography in healthy adults. *J Am Coll Cardiol*, 10(5):1032–9, 1987.

[172] Rossvoll O, Hatle LK. Pulmonary venous flow velocities recorded by transthoracic Doppler ultrasound: relation to left ventricular diastolic pressures. *J Am Coll Cardiol*, 21(7):1687–96, 1993.

[173] Goldstein JA, Barzilai B, Rosamond TL, Eisenberg PR, Jaffe AS. Determinants of hemodynamic compromise with severe right ventricular infarction. *Circulation*, 82(2):359–68, 1990.

Acknowledgments

This thesis would never have been possible without the help of many people. I would like to thank all who in different ways have helped me during the struggles towards my PhD.

My supervisor, Håkan Arheden, for recruiting me to Clinical Physiology and the cardiac MR group, teaching me cardiac physiology and cardiac MRI and for letting me to pursue my goals.

My co-supervisor, Martin Ugander, for helping me with writing the articles, sending me comments on manuscripts late at night and bringing overwhelming enthusiasm to the project.

Stig Lundbäck, for his pioneering works in the field of cardiac pumping and for inspiring the work that resulted in this thesis.

Peter Cain, for helping me through my first article.

Björn Jonson, for providing the academic environment of the Department of Clinical Physiology

Freddy Ståhlberg, for teaching me MR physics.

Einar Heiberg, for altering Segment whenever I need a new parameter.

The members of the cardiac MRI group for being great research partners and especially Henrik Engblom, Erik Hedström, Erik Bergvall and Karin Markenroth for helping me with graphs, Latex, MatLab and MR physics respectively.

The late Catharina Holmqvist, for teaching me cardiac MRI and supporting me during the first study of this thesis.

Ann-Helen Arvidsson and Christel Carlander for helping me with MRI acquisitions and keeping track of all papers.

Kerstin Brauer, Eva Hallberg, Märta Granbohm, Karin Larsson and Titti Owman for all help with teaching and courses, an important and fun part of scientific work.

Staff and colleagues at the Department of Clinical Physiology and the MR department, for understanding that research and clinical medicine are linked and support each other.

My parents, Ann-Marget and John Thomsen, Bengt Carlsson and my brothers and sister and their families, for loving me and believing in me.

My friends, for giving me other dimensions in life.

Lars, for love and companionship and for never complaining about the long hours.

The studies in this thesis were supported by grants from the Swedish Research Council, the Swedish Heart and Lung Foundation, Lund University, Faculty of Medicine and the Region of Scania.

Papers I–V